Autosomal Dominant-Hyper-IgE Syndrome patients contain pre-Th17-cells that are activated by opportunistic pathogens to produce IL-10

Giorgia Moschetti[1,2*], Chiara Vasco[1*], Francesca Clemente[1], Paola Larghi[1], Sara Maioli[3], Edoardo Scarpa[1,2], Elena Carelli[1], Nadia Pulvirenti[1], Maria Lucia Sarnicola[1], Mariacristina Crosti[1], Manal Bel Imam[4], Willem van de Veen[4], Loris Rizzello[1,2], Sergio Abrignani[1,3], Lucia A. Baselli[5], Rosa Maria Dellepiane[5], Maria Carrabba[6], Giovanna Fabio[6], Jens Geginat[1,3*]

[1] INGM, Fondazione Istituto Nazionale Genetica Molecolare "Romeo ed Enrica Invernizzi", Milan, Italy;
[2] Università degli Studi di Milano, Department of Pharmaceutical Sciences, Milan, Italy
[3] Università degli Studi di Milano, Department of Clinical Sciences and Community Health, Milan, Italy;
[4] Swiss Institute of Allergy and Asthma Research, Davos, Switzerland
5 Fondazione IRCCS Ca' Granda Ospedale Maggiore Policlinico, Pediatric Immunorheumatology Unit, ERN-RITA center, Milan, Italy.
[6] Fondazione IRCCS Ca' Granda Ospedale Maggiore Policlinico, Department of Internal Medicine, ERN-RITA center , Milan, Italy.

* Correspondence to: moschetti@ingm.org, vasco@ingm.org or geginat@ingm.org

We declare no conflict of interest

ABSTRACT

STAT3 is required for Th17-cell differentiation, and dominant-negative STAT3 mutations cause Autosomal Dominant-Hyper-IgE Syndrome (AD-HIES), which is characterized by a lack of Th17-cells and recurrent infections with opportunistic extracellular pathogens. T-cell responses to opportunistic pathogens in AD-HIES patients have however not been characterized. We previously identified an enigmatic population of IL-10 producing $CCR6^{+}$Th-cells that were largely non-polarised and lacked other subset-defining differentiation markers ("$CCR6^{single\text{-}positive(SP)}$"). Here we report that $CCR6^{SP}$T-cells are central memory T-cells (T_{CM}) that expressed the stemness-associated transcription factors LEF1 and TCF7, but also RORγt, the lineage-defining transcription factor of Th17-cells. Non-polarized $CCR6^{SP}$T-cells differentiated spontaneously to Th17-cells upon TCR stimulation, indicating that they were pre-committed to a Th17 fate. Spontaneous Th17 differentiation was promoted by an autocrine loop of STAT3-activating cytokines and inhibited by IL-4. IL-12 induced in addition IFN-γ, and consequently differentiation to Th1/17-cells. $CCR6^{+}$T-cells were strongly reduced in AD-HIES and Th17- and Tfh17-cells were hardly detectable. However, the residual $CCR6^{+}$T-cells contained Th1/17- and $CCR6^{SP}$T-cells that proliferated *in vivo*. They produced high amounts of IL-10, indicating that, unexpectedly, IL-10 production by human T-cells is STAT3-independent *in vivo*. Intriguingly, opportunistic pathogens selectively activated $CCR6^{+}$T-cells in AD-HIES patients to produce IL-10. Opportunistic bacteria and Mycobacterium tuberculosis induced in addition IL-2 and IFN-γ. We conclude that Th17 differentiation is not completely impaired in the absence of STAT3 signalling but arrested at an early stage of $CCR6^{+}T_{CM}$. These pre-Th17-cells produce IL-10 and require STAT3 to differentiate to Th17-cells and to fight extracellular pathogens but could directly generate Th1/17-cells to contain intracellular bacteria.

Significance

AD-HIES patients have impaired STAT3 signalling, lack consequently Th17-cells and experience recurrent infections with opportunistic extracellular pathogens. These patients were key to the dogma that Th17-cells control extracellular pathogens, but T-cell responses to these pathogens have surprisingly never been analyzed. Here, we report that Th17 differentiation in response to opportunistic extracellular pathogens in the absence of STAT3 signalling is arrested at an early stage of pre-Th17-cells that produce high levels of IL-10. These otherwise non-polarised T-cells acquired IFN-gamma production with IL-12 that could enable them to contain intracellular bacteria. These surprising findings demonstrates that Th17 differentiation is not completely blocked in the absence of STAT3 signalling, and that IL-10 production by human T-cells is STAT3-independent *in vivo*.

INTRODUCTION

CD4$^+$T-cells play a pivotal role to coordinate adaptive immune responses against pathogens. They acquire specialised functions upon priming in response to different classes of pathogens, in particular they acquire chemokine receptors and produce effector cytokines that enables them to home to the infected sites and to activate the appropriate effector arms of the immune response. Initially, Th1-cells that fight intracellular pathogens, including bacteria and viruses, and Th2-cells that contain extracellular parasites like helminths have been identified[1]. Th1-cells express the chemokine receptors CXCR3 and CCR5 and the lineage-defining transcription factor T-bet and they produce IFN-γ. Conversely, Th2-cells express CCR4 and CRTH2, express the lineage-defining transcription factor GATA3 and produce IL-4, IL-5 and IL-13. Later, subsets of Th17-cells and Tfh-cells have been identified that fight extracellular pathogens like bacteria and fungi and promote B-cell antibody responses, respectively, have been identified. Tfh effector cells express the transcriptional repressor BCL6, the chemokine receptor CXCR5 and produce IL-21[2]. Th17-cells express instead the transcription factor ROR-γt, the chemokine receptor CCR6, and produce the effector cytokines IL-17, IL-22[3,4] and GM-CSF[5]. Notably, CD4$^+$CCR6$^+$T-cells and Th17-cells are highly heterogeneous and contain several different subsets[1,6-8]. In humans, Th17-cells can be tacked according to CD161 expression[9], and Th17 effector cells express CCR5[10]. Moreover, a subset of human CCR6$^+$T-cells co-expresses CXCR3 and can produce both IFN-γ and IL-17[11] and are thus termed Th1/17-cells[12,13]. Another CCR6$^+$T-cell subset co-expresses CCR10 and produces IL-22, but not IL-17, suggesting that they represent Th22-cells[14,15]. Finally, a fourth CCR6$^+$T-cell subset co-expresses CXCR5, possesses B-helper functions and is called Tfh17[16].

Th1 and Th2 effector cells become memory cells that may persist long-term and provide protection upon re-infections. Also Th1 and Th2 memory cells are heterogeneous, and can in particular be sub-divided into central memory and effector memory T-cells (T_{CM} /T_{EM})[17]. T_{CM} are immature memory cells that express the stemness-promoting transcription factors TCF7/LEF1 as well as CCR7 and CD62L, which mediate homing to secondary lymphoid organs. They possess only low levels of effector functions, but expand efficiently upon antigenic re-stimulation, generating thus secondary waves of effector cells[17]. Conversely, T_{EM} have down-regulated CCR7 and CD62L and express instead chemokine receptors like CCR5, CCR9 or CCR10 that allows them to home rapidly to inflamed non-lymphoid organs like the skin or the gut. Since they possess high levels of effector cytokine producing capabilities, they can provide early protection. T_{CM} differentiate to T_{EM} upon TCR stimulation. We identified previously T_{CM} subsets expressing CXCR3 and CCR4 that differentiated preferentially to Th1 and Th2 effector cells, termed pre-Th1 and pre-Th2-cells[18]. These pre-committed T_{CM} subsets still retained the plasticity to differentiate to the opposing fate upon TCR activation in the presence of the appropriate polarizing cytokines. The key polarising cytokines that induce Th1 and Th2-cells, IL-12 and IL-4, activate the transcription factors STAT4 and STAT6, respectively. Conversely, Tfh-cells and Th17-cell differentiation is promoted by cytokines that signal via STAT3, like IL-6[19] and IL-21[20,21]. T_{FH}-cells in human blood have a T_{CM} phenotype, whereas Th17-cells contain both T_{CM} and T_{EM} subsets.

The role of STAT3 in human T-cell differentiation can be studied in patients with autosomal dominant Hyper IgE Syndrome (AD-HIES) that contain loss of function mutations in the STAT3 transcription factor that renders it inactive[22]. Aberrant transduction of STAT3 signalling coupled with its ubiquitous expression explain the multisystem manifestations of AD-HIES syndrome (OMIM 147060) including dermatitis, pulmonary disease, vasculopathy, and skeletal and connective tissue abnormalities. The triad of high levels of serum IgE, eczema and recurrent infections is the hallmark of this complex syndrome. Severe bacterial infection, cold abscess, osteomyelitis, chronic muco-candidiasis and

invasive fungal infections are very common signs[23]. AD-HIES patients lack IL-17 producing T-cells[24], and the opportunistic pathogens that cause recurrent infections like S. aureus and C. albicans are therefore believed to be controlled by IL-17[25].

We previously identified a population of $CCR6^{+}$T-cells with high IL-10 producing capacities[26], which possessed B helper activities. RNA sequencing indicated that they lacked canonical gene signatures of Tfh-cell and Th17-cells[27]. In human blood, these $CCR6^{+}$T-cells could be tracked as "CCR6 single-positive" ($CCR6^{SP}$) cells *ex vivo*, by excluding cells expressing differentiation markers of Th1/17-[11], Tfh17- [16] and Th17-cells[10,28]. They are increased in Systemic Lupus Erythematosus (SLE) patients and promote autoantibody production[27]. Here we show that these cells are T_{CM} that differentiate to Th17-cells upon TCR stimulation via an autocrine STAT3 signalling pathway. $CCR6^{SP}$T-cells are present in AD-HIES and produce IL-10 instead of IL-17 in response to opportunistic pathogens, suggesting that Th17 differentiation in the absence of STAT3 signalling is not completely impaired but rather arrested at a pre-Th17 state that is characterised by IL-10 production.

Material and Methods

Patients

All enrolled patients were diagnosed with AD-HIES according to the 2014 protocol by the Italian Primary Immunodeficiency Network (IPINet) group of the Italian Association of Pediatric Haematology Oncology (AIEOP) and this study patients are part of the Italian AD-HIES cohort previously described [29]. Each patients was analyzed for STAT3 mutations using Sanger sequencing or NGS. Table 1 summarises genetics and clinical features. During the study, all patients have been treated according to the IPINet protocol and their comorbidities managed according to the attending physicians' evaluation. Peripheral blood was isolated from patients with AD-HIES and age- and sex-matched healthy donors (HD). The local ethics committee approved this protocol study (1097_2019bis on 12/12/2019, experimental study protocol ID #1305). All the patients enrolled signed an informed consent form for this study, the genetic analysis and received genetic counselling. This study adhered to the ethical principles outlined in the Declaration of Helsinki and followed the guidelines of Good Clinical Practice.

Table 1 Patients' characteristics and infection history.

	Demographics		Genetics		Clinical characteristics	Past infections/cultures isolations during lifetime					
ID	sex	year of birth	molecular diagnosis	protein domain mutation	clinical events during lifetime	*C. albicans*	*S. aureus*	*A. fumigatus*	*S. pneumoniae*	*E. coli*	*M. tubercolosis*
#1	F	1969	STAT3 (c.1909 G>A, p.V637M)	SH2	Severe eczema, cold skin abscesses, recurrent bacterial pneumonias, pneumatoceles, bronchiectasies, chronic mucocandidiasis, basicranial aspergilloma at 54yo. Two lung lobectomies at 4yo and 12yo. Skeletal abnormalities.	+	+	+	-	-	-
#2	F	1974	STAT3 (c.1387_1389delGTG, p.V463del)	DNA-binding	Eczema, cold skin and recurrent breast abscesses, chronic mucocandidiasis. Skeletal abnormalities. Breast cancer.	+	+	+	-	-	-
#3	M	1993	STAT3 (c.1144 C>T, p.R382W)	DNA-binding	Eczema, cold skin abscesses, recurrent bacterial pneumonias, pneumatoceles, bronchiectasies, chronic mucocandidiasis. Lung lobectomy at 27yo. Skeletal abnormalities.	+	+	+	+	-	-
#4	M	1981	STAT3 (c.1699 A>G, p.N567D)	LINKER	Severe eczema, cold skin abscesses, recurrent bacterial pneumonias, pneumatoceles, bronchiectasies. Mucocandidiasis. Pulmonary fungal infection. Two lung lobectomies at 1yo and 8yo. Skeletal abnormalities. Allergic anaphylactic shock (nuts).	+	+	+	-	-	-
#5	M	1979	STAT3 (c.1144 C>T, p.R382W)	DNA-binding	Severe eczema, cold skin abscesses, osteomyelitis (twice), recurrent bacterial pneumonias, pneumatoceles, bronchiectasies, pulmonary aspergilloma, chronic mucocandidiasis, invasive pulmonary aspergillosis. Lung lobectomy at 18yo. Huge pelvic abscess needing radical removal of the prostate. Recurrent bacterial cholangitis. Skeletal abnormalities.	+	+	+	+	+	-
#6	F	1983	STAT3 (c.1139+1G>T, p.D371_G380del)	DNA-binding	Severe eczema, cold skin and recurrent breast abscesses, recurrent bacterial pneumonias, pneumatoceles, bronchiectasies, chronic mucocandidiasis. Lung lobectomy at 18yo out of aspergilloma. Skeletal abnormalities. Recurrent UTI. Neuroendocrine gastric displasia.	+	+	+	-	+	-

+: at least one documented infection during lifetime

-: no documented infection nor culture isolation

Isolation of human peripheral blood mononuclear cells

Human peripheral blood mononuclear cells (PBMCs) were isolated by density gradient centrifugation by Ficoll-Hypaque gradient (Amersham Pharmacia Biotech, Sweden). For characterization of T cell subsets from PBMCs, cells were stained with a combination of fluorochrome-conjugated antibodies as specified in supplementary Table 1 (sTable1) and sorted (FACSAria III, BD Biosciences), according to the expression of following specific surface markers combination: $CD4^{+}IL\text{-}7R^{+}CD25^{-}$

$CCR6^+CXCR3^+CXCR5^-$ (Th1/17 cells), $CD4^+IL\text{-}7R^+CD25^-CCR6^+CXCR3^-CXCR5^+$ (Tfh17 cells), $CD4^+IL\text{-}7R^+CD25^-CCR6^+CXCR3^-CD161^+$ and/or $CCR5^+$ (Th17 cells), $CD4^+IL\text{-}7R^+CD25^-CCR6^+CXCR3^-CD161^-CCR5^-$ ($CCR6^{SP}$); the latter subset was further subdivided according to CCR10 expression in $CCR6^+CCR10^+$ and $CCR6^{SP}$ ($CCR10^-$). Human monocytes were purified from healthy donors' PBMCs using anti-human CD14 magnetic microbeads and MACS cell separation columns (Miltenyi Biotec; Germany), according to the manufacturer's instructions.

Flow Cytometry

$CD4^+$T-cells were analyzed for the expression of surface markers, transcription factors, and cytokines by staining with various combinations of fluorochrome-conjugated monoclonal antibodies (**sTable 1**). Cells were stained using fixation with Intracellular Fixation & Permeabilization Buffer Set (Thermo Fisher Scientific, U.S.A.) to simultaneously detect surface markers, transcription factors, and cytokines, according to the manufacturer's instructions. Acquisition of stained cells was performed with a FACSymphony™ cytometer (Becton Dickinson, U.S.A.) and raw data were analyzed using FlowJo software version 10.8.1 (BD Biosciences).

Polyclonal stimulation of $CD4^+$T-cells to induce cytokine production

Purified T-cell subsets were incubated at 37°C for 2 hours in the presence or absence of phorbol 12-myristate 13- acetate (PMA, 50 ng/ml; Sigma Aldrich, U.S.A.), ionomycin (500 ng/ml; Sigma Aldrich, U.S.A.) in complete RPMI 1640 (10% FBS, 1 mmol/L sodium pyruvate, 10 mmol/L nonessential amino acids, and 1% penicillin/streptomycin), and with Brefeldin A (10 µg/mL; Sigma Aldrich, U.S.A.) for an additional 2 hours. After this 4-hour incubation period, cells were stained as before mentioned (flow cytometry section) and analyzed at the cytometer. IL-10 production was assessed also following 30 hours stimulation with immobilized anti-CD3 antibodies (5µg/ml; Biolegend, U.S.A.), supplemented with 10 ng/mL recombinant human IL-2 (rhIL-2, Miltenyi Biotec, Germany) with a an IL-10 secretion assay (Miltenyi Biotec; Germany) according to the manufacturer's instructions. Furthermore, the production of IL-10 by $CD4^+$ T-cells was assessed after 18 hours of stimulation of total PBMC with Staphylococcal enterotoxin B (SEB).

ELISA

The supernatants derived from anti-CD3/28-stimulated $CCR6^+$T-cell subsets were harvested, and subsequently stored at -80°C. Assessment of interleukin-6 (IL-6) production was performed using a commercially available kit (Biolegend, U.S.A.), following the manufacturer's prescribed protocols.

Immunofluorescence and imaging

Cells were fixed in 4% paraformaldehyde (PFA) for 10 min at room temperature and, after washing with PBS, blocking buffer (10% Fetal Calf Serum, FCS, in PBS) was added for 1h at room temperature. Cells were then washed with PBS and incubated with an anti-human CCR6 mouse monoclonal antibody (1:50, R&D Systems, U.S.A.) and an anti-CD4 rabbit monoclonal antibody (1:30, Abcam, UK) overnight at +4°C. Subsequently, cells were washed, and they were incubated with a chicken secondary antibody anti-mouse IgG Alexa Fluor™ 568 (1:1000, ThermoFisher Scientific, U.S.A.) and a goat secondary antibody anti-rabbit IgG Alexa Fluor™ 488 (1: 1000, ThermoFisher Scientific, U.S.A.) for 1 hour at room temperature.

Next, cells were washed with PBS, permeabilized using 0.1% Triton X-100 for 15 minutes, and they were incubated overnight with a rat anti-human IL-10 antibody (1:100, ThermoFisher, U.S.A). The following day, cells were washed with PBS and incubated with a donkey secondary antibody anti-rat IgG Alexa Fluor™ 647 secondary antibody for 1 hour at room temperature. After washing in PBS, cells were counterstained with DAPI (Molecular Probes, ThermoFisher Scientific, U.S.A.) and mounted using ProLong Diamond and ProLong Glass mounting reagents (both from ThermoFisher Scientific). Labeling control (sample section incubated in all the buffers and detergents used in the experiment, but not in secondary antibody) was performed before starting the experiments. The isotype control was included in each experiment. Fluorescence images were acquired using an inverted STELLARIS 8 Confocal Microscope (Leica Microsystems) equipped with a 405 laser and a tunable pulsed white light laser, utilizing a 40x air objective (numerical aperture [NA] 0.95) in three independent experiments. Quantification was performed using NIS-Elements V.5.30 software (Lim-Instruments). Ad-hoc designed pipelines of digital imaging analysis were implemented using the General Analysis 3 module of NIS-Elements to determine the intensity of fluorescence associated to the single cells present in the images.

Monitoring of functional IL-6 and IL-23 receptors according to STAT phosphorylation

The expression of functional IL-6 and IL-23 receptors (IL-6R and IL-23R) on CD4+ T-cells subsets was assessed by IL-6 and IL-23-induced STAT3 phosphorylation [20,30], respectively. Cells were incubated at 37°C for 30 minutes in the presence or absence of 10 ng/ml human recombinant IL-6 (Miltenyi Biotec, Germany) or IL-23 (Miltenyi Biotec, Germany) in RPMI 1640 (1 mmol/L sodium pyruvate, 10 mmol/L nonessential amino acids, and 1% penicillin/streptomycin) supplemented with 5% human serum (Euroclone S.p.A., Italy). Cells were then fixed and stained with a combination of fluorochrome-conjugated antibodies using Cytofix/Cytoperm Fixation/Permeabilization Buffer (BD Biosciences, U.S.A.) according to the manufacturer's instructions.

Th17 differentiation

$CCR6^{SP}$ and, as a control, $CCR6^{-}$T-cells were isolated from buffy coats of healthy donors and sorted based on their chemokine receptors expression as described previously [27]. In some experiments, $CCR6^{+}CXCR5^{+}$Tfh17-cells and $CXCR3^{+}CCR6^{+}$Th1/17-cells were also isolated as additional controls. In other experiments, $CCR6^{SP}$ and $CCR6^{-}$ FACS-sorted T cells were depleted from residual IL-17-, IFN-γ- or IL-22-producing cells with a cytokine secretion assay (Miltenyi, Germany). Cells were resuspended in complete RPMI 1640 (10% FBS, 1 mmol/L sodium pyruvate, 10 mmol/L nonessential amino acids, and 1% penicillin/streptomycin) and they were stimulated with PMA (50 ng/ml, Sigma Aldrich, U.S.A.) and ionomycin (500 ng/ml, Sigma Aldrich, U.S.A.) for 4h. Then, MACS® Cytokine Secretion Assays for IFN-γ or IL-22 and IL-17A (Miltenyi Biotec, Germany) were performed according to the manufacturer's instructions. Non-polarised $IL\text{-}17A^{-}/IFN\text{-}\gamma^{-}$ or $IL\text{-}17^{-}/IL\text{-}22^{-}$ $CCR6^{SP}$ and $CCR6^{-}$ T-cells were FACS-sorted and seeded in complete RPMI.

Cells were cultured in complete RPMI 1640 (10% FBS, 1 mmol/L sodium pyruvate, 10 mmol/L nonessential amino acids, and 1% penicillin/streptomycin) and stimulated with anti-CD3/28 coated-beads (Invitrogen, U.S.A. 1 to 1 concentration) for 6 days, in (i) the absence of exogenous Th17-promoting cytokines (ii) with 10ng/ml of human recombinant polarizing cytokines (i.e.,TGF-β, IL-4, IL-12; Miltenyi biotec, Germany) or WNT10a, (iii) in the presence of 10 ng/ml of anti-IL-6 (Biolegend, U.S.A.), anti- IL-10 (Miltenyi Biotec, Germany), 1μg/ml anti-IL-10R (R&D, U.S.A.) antibodies and sIL-21R (R&D, U.S.A.). After 6 days, cells were stimulated with PMA (50 ng/ml) and

237 ionomycin (500 ng/ml) in the presence of Brefeldin A (10 µg/mL), as previously described, and
238 stained as mentioned (flow cytometry section) and analysed for cytokine production at the cytometer.

239

240 **T-cell lines**

241 Total $CCR6^+$ and $CCR6^-$ or $CCR5^-CCR6^+$ and $CCR5^-CCR6^-T_{CM}$ were sorted from HIES patients and
242 healthy donors. Cells were then stimulated in vitro with irradiated allogeneic feeder cells and PHA (1
243 µg/mL, Sigma) in complete RPMI 1640 (10% FBS, 1 mmol/L sodium pyruvate, 10 mmol/L
244 nonessential amino acids, and 1% penicillin/streptomycin), supplemented with 200U/mL
245 recombinant human IL-2 (rhIL-2, Miltenyi Biotec, Germany). Fresh complete RPMI medium
246 supplemented with rhIL-2 was replaced every 6 days and T-cell lines were used for the experiments
247 (i.e., cytokine production following PMA ionomycin stimulation as previously described and RORγt
248 expression) 15 to 20 days after stimulation.

249

250 **Bioinformatic Analysis**

251 Flow cytometry data were imported into FlowJo software (version 10.8.0) to compensate for
252 fluorescence spreading; dead cells and debris were excluded from the analysis. To compare the blood
253 of three patients versus those of the same number of healthy donors a random down-sample of 6000
254 events for the $CD4^+$ T-cells compartment was performed. Finally, CD4+ T-cells down-sampled data
255 were merged and exported as an FCS file for further analysis in R software (version 4.0.2). Sample
256 batches were read using read.flowSet (2.6.0) from the flowCore R package. We applied the Logicle
257 transformation that allows multiple samples to estimate transformation parameters. To reduce batch
258 effect due to technical and not to biological variation we normalized the signal of each marker with
259 the function gaussNorm from the flowStat package (4.6.0). After the batch-specific pre-processing,
260 samples were concatenated into a SingleCellExperiment object in R using the function prepData from
261 the CATALYST R package (REF). Dimensionality reduction by UMAP was subsequently applied to
262 visualize the relative proximities of cells within reduced dimensions. We performed high-resolution,
263 unsupervised clustering and meta-clustering using FlowSOM (2.2.0) and ConsensusClusterPlus
264 (1.58.0) packages as reported previously [31]. The $CD4^+$ T-cell compartment was clustered based on
265 the expression of 13 markers: CD127, FOXP3, CD45RA, CCR7, CD27, CD62L, CCR5, CXCR3,
266 CCR6, CD161, CXCR5, CCR10 and CCR9. Manually annotated clusters were subsequently
267 visualized on the UMAP. Functional pseudo-time analysis to infer the differentiation trajectory of
268 cells was carried out by Diffusion Maps using the function run Diffusion Map on the
269 SingleCellExperiment object using default parameters.

270

271 **Antigen specificity assays**

272 Stimulation with heat-killed pathogens was performed for 3 hours with 10^6 PBMCs in RPMI 1640
273 complete medium (2mM glutamine, 1mM sodium pyruvate, 1% non-essential amino acids, 1%
274 penicillin/streptomycin) supplemented with 5% of Human Serum. Monensin (BD GolgiStop™, BD
275 Biosciences) was added for an additional 15 hours of incubation, and thereafter cells were analyzed
276 for the expression of CD69, IL-17A, IFN-γ, IL-2, and IL-10. Staphylococcus aureus (heat-killed S.
277 Aureus, HKSA), Streptococcus pneumoniae (heat-killed S. Pneumoniae, HKSP), Escherichia coli
278 (Heat killed E. coli (0111:B4 – InvivoGen), Candida albicans (heat-killed C. Albicans, HKCA) and
279 Mycobacterium tuberculosis (heat-killed M. Tuberculosis H37Ra, HKMT) were all purchased from

280 InvivoGen (U.S.A.) and used at the final concentration of 10^7 CFU/ml. Lipopolysaccharides (LPS,
281 Sigma Aldrich, U.S.A.) and Staphylococcal enterotoxin B (SEB, Sigma Aldrich, U.S.A.) were used
282 at concentrations of 200 ng/ml and 1 µg/ml, respectively. Stimulation of cells with peptide pools of
283 Candida albicans, Aspergillus fumigatus and Epstein Barr peptides was performed using 1 µg/ml of
284 PepTivator® C. albicans MP65, PepTivator® A. fumigatus SHMT, PepTivator® EBV Consensus
285 (Miltenyi Biotec, Germany), respectively. Viral, fungal, or bacterial antigens used in the antigen-
286 specificity assays are listed in Supplementary Table 2.

287

288 **Statistical analysis**

289 Statistical significance was evaluated using an unpaired Student t-test for the comparison of two
290 groups (with Mann-Whitney's or Welch's correction to analyze variables that were not normally
291 distributed) or by One way-ANOVA for comparison of more than two groups (Tukey's post hoc
292 correction). Significance was defined at p value < 0.05. Statistics were performed with Prism software
293 (version 7; GraphPad Software, Inc., La Jolla, CA, USA). Error bars report +/- SEM in all Figures.

294

295

296 **RESULTS**

297 **Human CCR6^{SP}T-cells represent an early stage of Th17 differentiation**

298 To map the differentiation stage of CCR6^{SP}T-cells in human blood of healthy donors, we first analysed
299 a panel of adhesion and chemokine receptors. All CCR6^{+}T-cell subsets, namely CCR6^{SP}, Th17-,
300 Th1/17- and Tfh17-cells, expressed high levels of CXCR4 and the β1-integrin (CD29, sFigure 1A).
301 CCR6^{SP}-T-cells expressed only low levels of gut-homing receptors (CCR9 and β7-integrin, Figure
302 1A), and completely lacked CXCR6 expression. Conversely, they expressed relatively high amounts
303 of the skin-homing receptors CCR4, CLA and of CCR10 (Figure 1A). Since CCR10 and CCR6 co-
304 expression is characteristic for human Th22-cells[1,14,15], we focussed the further analysis on CCR6^{SP}-
305 T-cells that lacked also CCR10. The features of the Th22-containing CCR10^{+} subset ("Th22") is
306 shown in the supplementary Figures 1 and 2. CCR6^{SP}T-cells and Tfh17-cells had a central memory
307 (T_{CM}) phenotype, since most cells co-expressed CCR7 and CD62L (Figure 1B, sFigure 1B).
308 Conversely, the majority of Th17-, Th1/17- and Th22-cells lacked either CCR7 or CD62L expression,
309 indicating that they were more differentiated and contained effector memory cells (T_{EM}). CCR6^{SP}-T-
310 cells expressed also high levels of the memory T-cell-associated marker CD27, whereas Th17- and
311 Th22-cells had partially down-regulated CD27. Finally, CCR6^{SP}-T-cells and Th22-cells lacked PD1
312 expression (Figure 1B, sFigure 1C), an inhibitory receptor induced by chronic T-cell activation.

313 RNA sequencing indicated that TCF7 and LEF1, transcription factors of the WNT pathway were
314 increased in CCR6^{SP}T-cells[27]. TCF7 and LEF1 promote stemness and are associated with poorly
315 differentiated T-cells. Consistently, they were highly expressed at the protein level in naïve and
316 CD45RA^{+}CCR7^{+}CD95^{+} memory stem cells (T_{SCM}), at intermediate levels in T_{CM} and at low levels
317 in T_{EM} (sFigure 1D). Among CCR6^{+}T-cells, Tfh17 and CCR6^{SP} T-cells expressed intermediate levels
318 of TCF7 and LEF1 (Figure 1C), consistent with their T_{CM} phenotype. Conversely, Th17-and Th1/17-
319 cells expressed low levels of TCF7 and LEF1, consistent with the presence of T_{EM}. We then analysed
320 expression of the transcription factor RORC/ROR-γt, which controls Th17-cell differentiation (Figure
321 1D). ROR-γt expression was as expected largely restricted to CCR6^{+}T-cells, and was highest in
322 CCR6$^{+}T_{EM}$ but it was clearly also expressed in CCR6$^{+}T_{CM}$ (sFigure 1E). Furthermore, it was
323 expressed at high level in Th17-cells and Th1/17-cells (Figure 1D), but relevant amounts were also
324 detectable in CCR6^{SP}, Th22- and Tfh17-cells.

325 T_{CM} produce only low levels of effector cytokines[17,18]. We assessed the cytokine producing capacities
326 of FACS-purified CCR6^{+}T-cell subsets following brief stimulation with PMA and Ionomycin (Figure
327 2A, sFigure 2A). Tfh17-, Th17- and Th1/17-cells displayed their well-established cytokine profiles.
328 Thus, Th1/17-cells produced the highest levels of IFN-γ, TNF, and GM-CSF and low levels of IL-
329 17[11,12]. Th17-cells produced instead the highest amounts of IL-17 and IL-22, intermediate levels of
330 TNF and GM-CSF and some IFN-γ[10]. Tfh17-cells produced in contrast only some TNF and were
331 largely unable to produce other effector cytokines. Also CCR6^{SP}T-cells produced TNF, but only low
332 levels of IFN-γ, IL-17, IL-22 and GM-CSF. Finally, Th22-cells produced high levels of GM-CSF and
333 TNF, low levels of IFN-γ and IL-22, but largely failed to produce IL-17 (sFigure 2A).

334 Since PMA plus Ionomycin stimulation is inefficient to induce IL-10 production in CCR6^{+}T-cells in
335 healthy individuals[26], we stimulated FACS-purified CCR6^{+}T-cell subsets with SEB-loaded
336 monocytes and assessed IL-10 production with immunofluorescence (Figure 2B, sFigure 2B). Under
337 these conditions, IL-10 was produced at high levels by CCR6^{SP}-T-cells and by Tfh17-cells, whereas
338 Th17-cells produced low levels.

339 IL-6R and IL-23R promote early and late Th17 differentiation, respectively[10,19,32,33]. We analysed the
340 expression of functional IL-23R on CCR6^{+}T-cell subsets according to IL-6/23R signalling. CCR6^{+}T-
341 cell subsets were shortly stimulated *ex vivo* with IL-23 or with IL-6, and tyrosine phosphorylation of
342 STAT1 and STAT3 analysed by flow cytometry as the readout[20] (Figure 2C, sFigure 2C). IL-6 induced
343 STAT1 and/or STAT3 phosphorylation in most Tfh17-cells, Th22-cells and CCR6^{SP}T-cells. Also
344 relevant fractions of Th17- and Th1/17-cells responded to IL-6, but in mean approximately half were
345 unresponsive. IL-23 responsiveness was in contrast overall low, but Th17-cells and Tfh17-cells
346 showed some IL-23 responsiveness, while CCR6^{SP}-T-cells responded only poorly, and Th22-cells
347 were largely unresponsiveness.

348 Overall, the characterization of CCR6^{SP}T-cells unveiled that they are IL-10 producing T_{CM} that
349 express only low levels of ROR-γt and Th17 effector cytokines, suggesting that they are at an early
350 stage of Th17 differentiation.

351

352 **TCR-activated CCR6^{SP}T-cells differentiate efficiently to Th17-cells in the absence of**
353 **polarising cytokines**

354 Since CCR6^{SP}T-cells expressed CCR6, ROR-γt and produced low levels of IL-17 we investigated if
355 they were pre-committed to a Th17 fate. To this aim we purified non-polarized CCR6^{SP}T-cells by
356 depleting the few CCR6^{SP}T-cells that produced IL-17, IFN-γ or IL-22 following stimulation with
357 PMA and Ionomycin with a cytokine secretion assay. The capacity to produce the same cytokines
358 was then analysed following *in vitro* culture for 6 days after brief re-stimulation with PMA and
359 Ionomycin. Strikingly, non-polarized CCR6^{SP}T-cells acquired high levels of IL-17 and IL-22
360 producing capacities under these conditions (Figure 3A, sFigure 3A, B), in spite of the fact that no
361 Th17-polarizing cytokines were added to the cultures. Notably, the latter is an absolute requirement
362 for Th17 differentiation of uncommitted helper T-cells[30]. Consistently, non-polarized CCR6^{-} control
363 cells largely failed to produce IL-17 or IL-22 under the same conditions. Moreover, when other
364 CCR6^{+}T-cell subsets were cultured for 6 days in the absence of Th17-polarising cytokines, CCR6^{SP}T-
365 cell produced significantly higher amounts of IL-17 as compared to Th1/17- and Tfh17-cells (Figure
366 3B). *In vitro* cultured CCR6^{SP}T-cells produced however only low levels of IL-10 (sFigure 3A),
367 suggesting that they switch spontaneously from IL-10 to IL-17/22 production.

368 To analyse the cytokine requirements of the "spontaneous" Th17 differentiation of CCR6^{SP}T-cells,
369 we first added cytokines that promote alternative T-cell fates. Production of IL-17 and IL-22 *by in*
370 *vitro* activated CCR6^{SP}T-cells was only weakly inhibited by TGF-β, but strongly and significantly by
371 IL-4 (Figure 3C, sFigure 3A). Induction of IL-17 was in contrast only weakly inhibited by WNT10A,
372 a soluble agonist of the WNT pathway that is expressed by CCR6^{SP}T-cells[27], activates LEF1/TCF7[34]
373 and may inhibit Th17 differentiation[35,36]. IL-12 had also an inhibitory effect on IL-17/IL-22 induction,
374 and strongly increased IFN-γ production in CCR6^{SP}T-cells (Figure 3C, sFigure3A). Consequently, it
375 promoted co-production of IFN-γ and IL-17, which is characteristic for Th1/17-cells[11,20,37], while IL-
376 4 was inhibitory.

377 Next, we asked if STAT3-activating cytokines produced by CCR6^{SP}T-cells, including IL-6 (sFigure
378 3C), IL-10[27] (Figure 2B) and IL-21[20] promoted spontaneous Th17 differentiation. FACS-sorted
379 CCR6^{SP}T-cells activated with anti-CD3 and anti-CD28 antibodies in the absence of exogenous
380 cytokines contained indeed high levels of phosphorylated STAT3 (Figure 3D). Moreover, STAT3
381 phosphorylation was significantly inhibited when IL-6, -10 and -21 were neutralized (Figure 3D, E).
382 Importantly, neutralising these STAT3-activating cytokines also significantly reduced IL-17 and IL-

22 production (Figure 3E, sFigure 3D), indicating that spontaneous Th17 differentiation was promoted by an autocrine loop of STAT3-activating cytokines.

In conclusion, CCR6^{SP}T-cells produce STAT3-activating cytokines upon TCR stimulation, which promote autocrine Th17 differentiation. However, CCR6^{SP}T-cells retain also a relevant degree of plasticity[6,38] and could be instructed by IL-12 to become Th1/17-cells.

CCR6^{+}T-cells are selectively reduced in AD-HIES.

To address the role of STAT3 in the biology of CCR6^{SP}T-cells *in vivo*, we then analyzed a cohort of AD-HIES patients, which have impaired STAT3 signalling and consequently lack Th17-cells[39]. Circulating CD4^{+}T-cells from DN-STAT3 patients were first compared to those obtained from three healthy donors (HDs) by multi-dimensional flow cytometry through unsupervised principal-component analysis (PCA, Figure 4A**)**. The visualization of cells in the space of the PCA revealed a distinct separation between the two cohorts, reflecting significant differences in the overall characteristics of CD4^{+}T-cells in HDs and AD-HIES. A more detailed analysis of the distinctive clusters associated with HDs or AD-HIES in CD4^{+}T-cell clusters are illustrated in a Unified Manifold Approximation and Projection (UMAP) analysis (Figure 4B**)**. Details about the marker expression in individual clusters and in the UMAP are shown in supplementary Figure 4A-C. Notably, cells in cluster 9 displayed the phenotype of CCR6^{SP}T-cells, whereas Clusters 11 and 13 corresponded to CCR6^{+}CCR10^{+} Th22$_{CM}$ and T_{EM}, respectively. Moreover, clusters 7 and 14 contained, respectively, T_{CM} and T_{EM} of Th17-cells together with Th1/17-cells. AD-HIES patients exhibited a selective reduction of all five CCR6^{+}T-cell clusters (Figure 4C), that was mainly compensated by an increase of naïve T-cells (Cluster 1, Figure 4C). Notably, two Th1 clusters (Clusters 6, 16) were instead largely unchanged. Manual gating confirmed an increase of naïve T-cells in HIES (sFigure 4D). Conversely, the frequencies of Th1, Th2 and regulatory T-cell subsets, i.e. FOXP3^{+}Tregs and EOMES^{+}Tr1-like cells[40], were similar to healthy donors (sFigure 4E). Finally, we performed Diffusion map analysis, which predicts hypothetical T-cell differentiation pathways in pseudotime. The Diffusion map suggested a progressive differentiation from naïve to effector T-cells, with T_{CM} and T_{EM} being early and late differentiation intermediates, respectively (Figure 4D). Furthermore, the diffusion map was consistent with a relatively immature differentiation stage of CCR6^{SP}T-cells, positioning them between T_{FH}- and other T_{CM} clusters.

Residual CCR6^{+}T-cells in AD-HIES patients contain Th1/17-cells and CCR6^{SP}T-cells that produce increased amounts of IL-10

Conventional gating of the flow cytometry data analysis confirmed that AD-HIES patients exhibit a reduction of all CCR6^{+}T-cell subsets (Figure 5A**)**. Notably, however, while Th17- and Tfh17 subsets were hardly detectable at all in AD-HIES, Th1/17-cells and CCR6^{SP} were only partially reduced, suggesting that STAT3 signalling is not an absolute requirement for their generation. Consequently, when the relative contributions of subsets to CXCR3^{-}CCR6^{+}T-cells was analysed, most cells displayed a CCR6^{SP} phenotype in AD-HIES patients (Figure 5A**)**. Consistently, CCR6^{+}T-cells in AD-HIES patients contained higher frequencies of T_{CM} (Figure 5B), expressed higher levels of LEF1/TCF7 (Figure 5C) and lower levels of ROR-γt as compared to CCR6^{+}T-cells from HDs (Figure 5D). However, CCR6^{+}T-cells in AD-HIES patients expressed slightly increased levels of skin- and gut-homing receptors (Figure 5E), possibly in response to recurrent infections at barrier organs. Statistical significance was reached for CCR9. Conversely, the β1-Integrin CD29 was significantly

427 reduced on CCR6$^+$T-cells in AD-HIES patients. Finally, CD27 and CCR5 expression on CCR6$^+$T-
428 cells in AD-HIES patients was similar to those from healthy donors (sFigure 5A, B).

429 We then analysed the cytokine producing capacities of CCR6$^+$T-cells in AD-HIES patients after brief
430 stimulation with PMA and Ionomycin. They largely lacked IL-17 producing capacities as expected,
431 but expressed normal levels of IFN-γ, IL-2, IL-4, IL-21, TNF and GM-CSF (Figure 6A and sFigure
432 6A**).** Interestingly, CCR6$^-$T-cells in AD-HIES patients expressed however significantly higher levels
433 of IL-2. Surprisingly, CCR6$^+$T-cells in AD-HIES patients produced significantly increased levels of
434 IL-10 (Figure 6B**)**. Notably, IL-10 production by CCR6$^-$T-cells, as well as FOXP3$^+$Tregs and
435 EOMES$^+$Tr1-like cells[40] was instead comparable in AD-HIES patients and HDs (sFigure 6B). Since
436 CCR6$^+$T-cells have peculiar stimulation requirements for IL-10 production[41], we analysed IL-10
437 production also after stimulation of the TCR of purified T-cell subsets with anti-CD3 antibodies in
438 the presence of IL-2[26], and upon stimulation of total PBMC with the superantigen SEB, which induces
439 a productive interaction between the TCR and MHC class-II molecules. Also under these more
440 physiological activation conditions CCR6$^+$T-cells in patients with AD-HIES produced significantly
441 higher amounts of IL-10 as compared to CCR6$^+$T-cells in healthy donors, and also as compared to
442 CCR6$^-$T-cells in the same patients (Figure 6B).

443 We next analysed if CCR6$^+$T-cells in DN-STAT3 could differentiate to Th17-cells spontaneously *in*
444 *vitro*, as is characteristic for CCR6^{SP}T-cells in STAT3-sufficient donors (Figure 3A). To this aim we
445 generated T-cell lines with CCR6$^+$ and CCR6$^-$T-cells from AD-HIES patients and healthy donors.
446 Some lines were sorted CCR5$^-$ (sFigure5B) to exclude T_{EM}[10,12,17]. Total CCR6$^+$ and CCR5$^-$CCR6$^+$$T_{CM}$
447 lines from AD-HIES patients expressed normal amounts of IFN-γ, but, as expected, significantly
448 lower levels of IL-17 and ROR-γt as compared to CCR6$^+$T-cell lines from healthy donors (Figure
449 5C). Notably, however, CCR6$^+$T-cells from AD-HIES patients did produce some IL-17, and this IL-
450 17 production reached statistical significance as compared to CCR6$^-$T-cell lines from the same
451 patients. Thus, although spontaneous Th17 differentiation was strongly reduced, it was not
452 completely impaired in AD-HIES patients, suggesting that CCR6$^-$T-cells from HIES patients may
453 acquire some protective effector functions upon *in vitro* expansion.

454 Finally, we analysed the *ex vivo* expression of activation and proliferation-associated markers. T-cells
455 in AD-HIES patients expressed in general higher levels of PD1. Moreover, selectively CCR6$^+$T-cells
456 had upregulated CD69 and expressed also significantly higher levels of Ki67 as compared to
457 CCR6$^+$T-cells in healthy donors, and as compared to CCR6$^-$T-cells in AD-HIES patients, indicating
458 that they had recently divided *in vivo* (Figure 6D).

459 In conclusion, CCR6$^+$T-cells in AD-HIES patients are reduced, but not absent and contain CCR6^{SP}T-
460 cells. Moreover, they are activated *in vivo* and produce increased amounts of IL-10.

461

462 **CCR6$^+$T-cells in AD-HIES are activated by opportunistic pathogens to produce IL-10**

463 Patients with AD-HIES are characterised by recurrent infections with opportunistic pathogens, in
464 particular all patients experienced infections with Staphylococcus aureus, Candida albicans and
465 Aspergillus fumagatus (Table 1), which are normally controlled by IL-17 producing T-cells[11]. In
466 addition, a minority of patients experienced infections with Escherichia coli and/or Streptococcus
467 pneumoniae. Conversely, infections with Mycobacterium tuberculosis were never diagnosed,
468 although patients were not vaccinated. We analysed if CCR6$^+$T-cells in AD-HIES responded to these
469 pathogens, which all activate preferentially CCR6$^+$T-cells in healthy individuals. To this aim we
470 stimulated cells with a panel of heat-killed pathogens and analysed pathogen-induced cytokine

471 production by $CD4^+CCR6^+$ and $CCR6^-$T-cell subsets. $CCR6^+$T-cells from AD-HIES patients
472 produced significantly higher amounts of IL-2 and IFN-γ as compared to $CCR6^+$T-cells from healthy
473 donors in response to Escherichia coli[10], Streptococcus pneumoniae and Mycobacterium
474 tuberculosis[11] (Figure 7A). Only $CCR6^+$T-cells from STAT3-sufficient healthy donors produced in
475 contrast IL-17 to all tested pathogens. Notably, $CCR6^+$T-cells from AD-HIES patients produced in
476 contrast very high amount of IL-10 that reached statistical significance in response to nearly all
477 pathogens. As expected, heat-killed pathogens increased the T-cell stimulatory capacities of antigen-
478 presenting cells ($CD14^+$monocytes, sFigure 7A). Although stimulation with LPS activated monocytes
479 to a similar extend and increased the expression of CD69 on T-cells (sFigure 7B), it failed to induce
480 T-cell cytokine production, suggesting that the cytokines were induced by pathogen-derived antigens.
481 Consistently, also $CCR6^-$T-cells up-regulated CD69 with LPS (sFigure 7B), but largely failed to
482 produce cytokines with heat-killed pathogens (sFigure7C).

483 Tu further exclude an unspecific activation of $CCR6^+$T-cells by heat-killed pathogens, we analysed
484 T-cell responses to commercially available antigenic peptide pools derived from selected pathogens,
485 i.e. C. albicans (MP65) and Aspergillus (SHMT). Responses to EBV (immunodominant peptide
486 pool), which preferentially activates $CCR6^-$T-cells[12], were analysed as control. Consistent with the
487 results obtained with heat-killed Candida, we observed only low IL-2 and IFN-γ responses (sFigure
488 7D), but we were again able to detect a switch from IL-17 to IL-10 production of pathogen-specific
489 $CCR6^+$T-cells in AD-HIES (Figure 7B). The increased IL-10 production in response to MP65 in AD-
490 HIES patients reached statistical significance. $CCR6^-$T-cells largely failed to respond also to these
491 peptide antigens (sFigure 7D) However, they showed a significant IFN-γ response to EBV-derived
492 peptides (Figure 7C, sFigure 7E), indicating that EBV-specific Th1-cells were generated normally in
493 AD-HIES patients[12].

494 In conclusion, $CCR6^+$T-cells are specifically activated by bacteria and fungi, including those causing
495 recurrent infections in AD-HIES. However, they produce IL-10 instead of IL-17 in AD-HIES patients,
496 consistent with the view that pathogen-specific $CCR6^+$T-cells are arrested at a pre-Th17 stage in the
497 absence of STAT3 signalling.

498

499

Discussion

Th17-cells produce IL-17, express the lineage-defining transcription factor ROR-γt and the chemokine receptor CCR6[3,32]. They are heterogeneous and contain different pro- and anti-inflammatory subsets[7,8]. We mapped here the differentiation stage of a population of human IL-10 producing CCR6$^+$T-cells that produced only low levels of IL-17. We showed previously that IL-10 producing CCR6$^+$T-cells could inhibit autoreactive T-cell proliferation in a partially IL-10-dependent manner[26]. They had however a context-dependent regulatory/helper function and could also induce IgG production from naïve B-cells in a partially IL-10-dependent fashion[27]. Notably, these CCR6$^+$ helper T-cells are unrelated to EOMES$^+$Tr1-like cells, which also produce IL-10 but do not express CCR6 and are probably generated from Th1-cells upon chronic TCR stimulation[40,42-45]. Here, we showed that CCR6$^+$T-cells that lack differentiation markers of established CCR6$^+$T-cell subsets (CCR6^{SP}) and produce IL-10 represent an early stage of Th17 differentiation, since they displayed a T_{CM} phenotype but expressed nevertheless some ROR-γt, suggesting that they are pre-committed to a Th17 fate. Consistently, TCR stimulation was sufficient to induce Th17-cells. This "spontaneous" Th17 differentiation was fast, highly efficient and occurred in the absence of exogenous Th17-promoting cytokines. Notably, in uncommitted human helper T-cells, i.e. naive CD4$^+$T-cells that lack CCR6 expression, Th17 differentiation is in contrast slow, inefficient and requires a combination of several Th17-promoting cytokines, i.e. IL-1β, IL-6, IL-23 and low levels of TGF-β[30]. Thus, CCR6^{SP} are pre-committed to a Th17 fate and represent thus pre-Th17-cells, in analogy to the pre-Th1- and pre-Th2 central memory cells that we have identified previously[18]. A feature of these pre-committed T_{CM} subsets is that they can generate spontaneously effector cells of their respective lineage, but that they retain nevertheless a relevant degree of plasticity to differentiate to alternative fates upon instruction by polarising cytokines. In the case of pre-Th17-cells, IL-12 induced IFN-γ, and promoted thus the differentiation to Th1/17-cells.

STAT3 signalling has a non-redundant role in Th17 differentiation, as evidenced by the absence of IL-17 producing T-cells in AD-HIES patients with DN-STAT3 mutations[24,39,46], and in mice with genetic defects in STAT3 activation[47]. Naïve T-cells developing into Th17-cells activate STAT3 initially in response to IL-6, which then induces IL-21 production to amplify STAT3 activation and Th17 differentiation in an autocrine feed-forward loop[19,48,49]. Terminal Th17 differentiation is induced by IL-23, which also signals via STAT3. Notably, however, CCR6 and ROR-γt in human CD4$^+$T-cells may be induced initially by TGF-β, which does not activate STAT3 and inhibits IL-17 induction in the absence of STAT3 signalling[26,50]. Once induced, CCR6 expression in human CD4$^+$T-cells is largely stable[51]. Thus, pre-Th17-cells may be generated in response to TGF-β, which could also promote IL-10 production[48]. The strongly reduced spontaneous Th17 differentiation of CCR6$^+$T-cells from patients with AD-HIES indicated that STAT3 signalling was indeed critical. However, the residual IL-17 production of *in vitro* cultured CCR6$^+$T-cells from AD-HIES patients suggested that also a STAT3-independent pathway may contribute[52]. In any case, our results indicate that CCR6$^+$ helper T-cells switch progressively from IL-10 to IL-17 production upon Th17 differentiation. This is surprising, because previously the opposite has been documented, i.e. that IL-17-producing Th17 effector cells switch to IL-10 production, trans-differentiating to regulatory T-cells upon resolution of inflammation in response to TGF-β[53,54]. Indeed, human CCR6$^+$T-cell clones could switch from IL-17 to IL-10 and back to IL-17 production upon *in vitro* activation[7,55]. It should however be noted that IL-10 produced by pre-Th17-cells and regulatory T-cells has apparently different functions and at different sites *in vivo*, i.e. induction of IgG by B-cells in secondary lymphoid organs and inhibition of inflammation in the intestine, respectively.

Inborn errors of immunity unveil non-redundant factors of the immune defence against pathogens. Patients with AD-HIES lack IL-17 producing T-cells and experience, presumably as a consequence, recurrent infections with opportunistic extracellular pathogens[25,56]. However, the presumably aberrant T-cell response to these opportunistic pathogens have not been investigated yet. It is also possible that protective T-cells are generated, but are unable to migrate to the infected tissues. Our results suggest that the expression of skin- and gut-homing receptors on T-cells is largely STAT3-independent, with the noticeable exception of the β1-integrin CD29 that was selectively reduced on CCR6$^+$T-cells. The requirements of T-cell migration to the lung, which is frequently affected by infections in AD-HIES patients, are however less well-defined, but β1-integrins appear to play a role[57]. Consistent with a key role for Th17 differentiation, however, also patients with deficient ROR-γ expression fail to control C. albicans and S. aureus, and they experience in addition uncontrolled infections with the intracellular bacterium M. tuberculosis[58]. The latter is controlled by Th1/17-cells[11], which express ROR-γt and produce high levels of IFN-γ. The fact that M. tuberculosis is controlled in AD-HIES patients could thus be attributed to the residual Th1/17-cells. Consistently, M. tuberculosis-stimulated CCR6$^+$T-cells from AD-HIES patients produced high levels of IFN-γ, that could activate macrophages to kill the intracellular pathogen. The M. tuberculosis-specific T-cells produced also high amounts of IL-10, but since IL-10 signals via STAT3 it is probably unable to inhibit macrophage functions in AD-HIES patients[59]. Our *in vitro* differentiation experiments suggested further that Th1/17-cells may be directly derived from pre-Th17-cells with IL-12, without the need to differentiate first to Th17-cells. Alternatively, they may be derived from Th1-cells[60], but this alternative pathway is induced by TGF-β and IL-6, and therefore likely to be impaired in the absence of STAT3 signalling. Also E. coli, which could induce Th17-cells in the gut[10], strongly activated CCR6$^+$T-cells in AD-HIES to produce IL-2, IL-10 and IFN-γ. Two of the AD-HIES patients had nevertheless documented, disseminated infections with E. coli (Table 1), suggesting that this response is suboptimal. Most important, also the opportunistic pathogens that cause recurrent infections in all AD-HIES patients activated strongly and selectively the residual CCR6$^+$T-cells, and consistently induced IL-10 instead of IL-17. S. aureus-specific IL-10 producing Th17-cells are present in healthy individuals[7], but evidence from mice suggests that they are indeed not protective[54]. The increased IL-10 production by CCR6$^+$T-cells in AD-HIES patients was nevertheless surprising, since IL-10 production in developing Th17-cells is promoted by IL-6 and IL-21[38,48], and IL-21-induced IL-10 production by T-cells *in vitro* is defective in AD-HIES patients[61]. Our results indicate however that STAT3 is not required for IL-10 production by neither helper nor regulatory T-cells *in vivo*. Indeed, it is known that T-cell IL-10 production could also be induced by IL-4 or IL-12 via STAT4 or STAT6, respectively[62]. Moreover, a presumably STAT3-independent inducer of IL-10 is chronic TCR stimulation. The continuous activation of CCR6$^+$T-cells by opportunistic pathogens, presumably in the presence of constitutively available TGF-β[63], may thus be responsible for the aberrantly high IL-10 production by CCR6$^+$T-cells in AD-HIES.

In conclusion, AD-HIES-associated opportunistic pathogens induce pre-Th17-cells that are continuously activated to produce IL-10, but that cannot differentiate to Th17-cells in the absence of STAT3 signalling and consequently lack protective functions. However, they can generate Th1/17-cells in response to IL-12 that could contain intracellular pathogens like M. tuberculosis. The specificity for opportunistic pathogens and the residual IL-17 production of CCR6$^+$T-cells derived from AD-HIES patients suggests that autologous adoptive T-cell transfer may be a future therapeutic strategy to improve the control of infections.

ACKNOWLEDMENTS

This work was supported by the Telethon Foundation, grant n. GGP19323 and by the Italian Ministry of instruction, University and Research PRIN 2022 Project P20228W4FJ

595 **FIGURE LEGENDS**

596

597 **FIGURE 1: CCR6^{SP}-T-cells have a central memory phenotype**

598 **A:** Frequencies of CXCR6, CCR4, CCR9, CCR10, Integrin(ITG)-β7 and CLA expression were
599 measured *ex vivo* by surface staining of gated CCR6^{+}CD4^{+}T-cells subsets from peripheral blood
600 (n=7).

601 **B:** Co-expression of CD62L/CCR7 (stacked histograms, left), expression of CD27 (centre) and PD1
602 (right, n=7).

603 **C:** Co-expression of TCF7/LEF1 (stacked histograms) were measured *ex vivo* by intracellular
604 staining of gated CCR6^{+}CD4^{+}T-cell subsets (n=7)

605 **D:** RORC/γt expression in CCR6^{+}CD4^{+}T-cell subsets (n=5).

606 **A-D:** Statistical significance was calculated using One-way ANOVA and reported as *p< 0.05, **p<
607 0.01, ***p< 0.001.

608

609 **FIGURE 2: CCR6^{SP} T-cells can produce high amounts of IL-10, but only low levels of Th1/17**
610 **effector cytokines**

611 **A:** Frequencies of IFN-γ, TNF-α, GM-CSF (bar histograms) expression and co-expression of IL-
612 17A/IL-22 (stacked histograms) of *ex vivo* FACS-purified, stimulated CCR10^{-}CCR6^{SP}, Th17, Th1/17
613 and Tfh17 subsets from peripheral blood (n=4).

614 **B**: IL-10 production was assessed in the indicated purified CCR6^{+}T-cell subsets stimulated with
615 monocytes and SEB for 16 hours by immunofluorescence. Shown is the FI of IL-10 and the mean
616 percentages of IL-10^{+} cells among CCR10^{-}CCR6^{SP}, Th17- and Tfh17-cells from three different
617 donors. Also a representative image with IL-10^{+}CCR6^{SP}T-cells is shown.

618 **C:** STAT1/3 phosphorylation (pSTAT1/3) of *ex vivo* stimulated CCR10^{-}CCR6^{SP}, Th17, Th1/17 and
619 Tfh17 cells in response to IL-6 and IL-23 to assess the expression of functional IL-6R and IL-23R,
620 respectively. Unstimulated cells are shown as negative control. Statistical significance was calculated
621 using One-way ANOVA and reported as *p< 0.05, **p< 0.01, ***p< 0.001.

622

623 **FIGURE 3: IL-10 produced by TCR-activated CCR6^{SP} T-cells promotes Th17 differentiation**

624 **A.** FACS-purified CCR6^{SP} T-cells or CCR6^{-} control cells were stimulated *ex vivo* and depleted from
625 IL-17 and IFN-γ (n=4) or IL-17 and IL-22 producing cells (n=3) with a cytokine secretion assay by
626 cell sorting. Cells were cultured with anti-CD3/28-coated beads and were restimulated after 6 days
627 cells with PMA and Ionomycin. The induction of the previously depleted cytokines was analyzed by
628 intracellular staining. Left: Dot plots of IL-17 and IL-22 induction in one representative donor. Right:
629 Bars report the frequencies of induced cytokine-producing cells. IL-17^{+} and IFN-γ^{+}-depleted cells are
630 indicated by filled circles, IL-17^{+} and IL-22^{+} depleted cells by triangles. Statistical significance for
631 each cytokine was calculated with a paired student's t-test.

632 **B.** IL-17 production by the indicated T-cell subsets cultured for 6 day with anti-CD3/28-coated beads
633 induced by restimulated with PMA and Ionomycin. Statistical significance was calculated with One-
634 way ANOVA.

635 **C.** FACS-purified $CCR6^{SP}$ T-cells were cultured for 6 day with anti-CD3/28-coated beads in the
636 absence or presence of the indicated agonists were analyzed for IL-17 and IFN-γ producing capacities.
637 **D/E:** FACS-purified $CCR6^{SP}$ T-cells were cultured with anti-CD3/28-coated beads in the absence or
638 presence of the indicated antagonists and analyzed for STAT3 phosphorylation after 24 hours or for
639 IL-17 and IL-22 production after 6 days following brief restimulation with PMA and Ionomycin.

640 **C, E:** Shown is the fold-change as compared to $CCR6^{SP}$T-cells stimulated with anti-CD3/28 beads
641 alone (indicated by dotted lines). Statistical significance for each condition was calculated with a
642 paired student's t-test and is indicated by */**/***/**** on the top of the columns.

643

644 **FIGURE 4: Unbiased analysis of the $CD4^+$T-cell compartments of AD-HIES patients unveils a**
645 **selective decrease of $CCR6^+$T-cell clusters**

646 **A.** Principal Component Analysis of 3 AD-HIES patients and 3 healthy donors (HDs), respectively
647 coloured in blue and in red. Number in the label indicated the sample IDs.

648 **B.** UMAP maps of the 16 identified $CD4^+$T-cell clusters marked with different colours in the blood
649 of HD and AD-HIES patients.

650 **C.** Bar-plots showing cluster distributions in the blood of HD and AD-HIES patients.

651 **D.** Possible cell differentiation pathways of the 16 identified $CD4^+$T-cell clusters was inferred by
652 Diffusion Map analysis.

653 **B-D)** Colour code and phenotypes of the 16 clusters are indicated in the Figure.

654

655 **FIGURE 5: Residual $CCR6^+$T-cells cells in AD-HIES patients contain pre-Th17- and Th1/17-**
656 **cells**

657 **A:** Upper bar histograms show the frequencies of $CCR6^{SP}$, Th17, Th1/17 and Tfh17-cells among
658 $CD4^+$T-cells in healthy donors (HD, blue bars, n=7) and AD-HIES patients (red bars, n=6). Statistical
659 significance was calculated using paired t-test and reported as * $p < 0.05$, ** $p < 0.01$. Lower pie
660 charts show the relative contributions of Tfh17-cells, Th17-cells and $CCR6^{SP}$T-cellst to $CXCR3^-$
661 $CCR6^+$T-cells.

662 **B:** Co-expression of CD62L and CCR7 in gated $CCR6^+$ and $CCR6^-CD4^+$T-cells of HD (n=8) and
663 AD-HIES patients (n=4).

664 **C.** Intracellular LEF1 and TCF7 co-expression of gated $CCR6^{+/-}$T-cells from AD-HIES patients (n=5)
665 and HD (n=5).

666 **D:** Intracellular RORC/γt expression was measured ex vivo in gated $CCR6^{+/-}$T-cells and $CCR6^-$T-
667 cells of HD (blue bars, n=9) and AD-HIES patients (red bars, n=4).

668 **E:** Frequencies of ex vivo CCR10, CLA, CCR9, Integrin(ITG)-β7, PD1 and CD29 (ITG-β1)
669 expression among $CCR6^+$ and $CCR6^-CD4^+$T-cells of HD (blue bars, n=7-8) and AD-HIES patients

670 (red bars, n=4-6). **B-E:** Statistical significance was calculated using One-way ANOVA and reported
671 as *p< 0.05, **p< 0.01, ***p< 0.001.

672

673 **FIGURE 6: CCR6$^+$T-cells in AD-HIES patients are activated *in vivo* and produce increased**
674 **amounts of IL-10**

675 **A:** Frequencies of IL-17A, IFN-γ, IL-2, IL-4 and IL-21 expressing cells among CCR6$^+$ and CCR6$^-$T-
676 cells stimulated *ex vivo* with PMA and Ionomycin obtained from AD-HIES patients (red bars, n= 4-
677 6) and HD (blue bars, n=7).

678 **B:** Left: Frequencies of IL-10 producing cells among CCR6$^+$ and CCR6$^-$T-cells from AD-HIES
679 patients (red bars, n=4) and HD (blue bars, n=7) following 4 hours of stimulation with PMA plus
680 Iomomycin. Centre: Frequencies of IL-10-producing cells after 30h stimulation with anti-CD3
681 antibodies and IL-2 of CD4$^+$T-cell subsets sorted according to CCR6 expression from AD-HIES
682 patients (red bars, n=4) and healthy donors (blue bars, n=6). Right: Frequencies of IL-10 producing
683 cells among superantigen (SEB)-stimulated, gated CCR6$^+$ and CCR6$^-$T-cells from AD-HIES patients
684 (red bars, n=5) and HD (blue bars, n=7).

685 **C:** Expression of IL-17A (left), IFN-γ (centre) and RORyt (right) in T-cell lines derived from FACS-
686 purified total CD4$^+$CCR6$^+$ (yellow dots) or CCR5$^-$CD4$^+$CCR6$^+$T$_{CM}$-cells (blue/red dots) from HD
687 (blue bars, n=6-7) and AD-HIES patients (red bars, n=4-6).

688 **D:** *Ex vivo* expression of PD1 (left), CD69, (center) and Ki67 (right) in CCR6$^+$ and CCR6$^-$T-cells
689 from AD-HIES patients (red bars, n= 6) and HD (blue bars, n=7). **A, B and D**: Statistical significance
690 was calculated using One-way ANOVA and reported as *p< 0.05, **p< 0.01, ***p< 0.001. **C**:
691 Statistical significance was calculated using Wilcoxon paired test and reported as *p<0.05.

692

693 **FIGURE 7: CCR6$^+$T-cells in AD-HIES patients are activated by opportunistic pathogens to**
694 **produce IL-10, but not IL-17**

695 **A.** Co-expression of CD69 and IFN-γ (upper left panel), IL-2 (upper right panel), IL-17A (lower left
696 panel) and IL-10 (lower right panel) in CD4$^+$CCR6 T-cells from AD-HIES patients (red bars, n=5)
697 and HD (blue bars, n=8) stimulated *ex vivo* with the indicated pathogens. CTR: cells incubated
698 without a heat-killed pathogen was analysed as negative control. Statistical significance was
699 calculated using paired t-test and reported as * p < 0.05, ** p < 0.01 on a bracket for significant
700 differences between HDs and AD-HIES patients, and as ° or °° on the columns for significant
701 responses as compared to the negative control.

702 **B.** Co-expression of CD69 and the indicated cytokines in CCR6$^+$T-cells from AD-HIES patients (red
703 bars, n=4) and HD (blue bars, n=6) induced by overlapping peptide pools derived from Candida
704 albicans (MP65) or from Aspergillus fumagatus (AMT). A/B: Unstim: Cells incubated without
705 peptides were analysed as negative control.

706 **C.** Co-expression of CD69 and IFN-γ in CCR6$^-$T-cells from AD-HIES patients (red bars, n=5) and
707 HD (blue bars, n=7) induced by an immune-dominant peptide pool derived from EBV.

708

709

710 SUPPLEMENTARY FIGURE 1:

711 **A**: Frequencies of CXCR4 (left) and CD29 (right) expression measured *ex vivo* by surface staining
712 on gated $CCR6^{+}$T-cell subsets. **B**: Co-expression of CD62L/CCR7, **C**: expression of CD27 and PD1,
713 D: Co-expression of TCF7/LEF1 (stacked histograms) and **E**: RORγt (histogram bars) among
714 $CCR6^{+}$T-cells gated as $CCR10^{+}TH22$ or $CCR10^{-}CCR6^{SP}$. A/B: Statistical significance was calculated
715 using paired t-test and reported as * $p < 0.05$, ** $p < 0.01$. **D**: Stacked histogram show co-expression
716 of TCF7/LEF1 in naïve ($CD45RA^{+}CCR7^{+}CD95^{-}$), T_{SCM} ($CD45RA^{+}CCR7^{+}CD95^{+}$), T_{CM} and T_{EM} as
717 internal control. **E**: RORγt expression in $CCR6^{+/-}$ naïve ($CCR7^{+}CD45RA^{+}$), central ($CCR7^{+}CD45RA^{-}$
718 , T_{CM}) and effector memory ($CCR7^{-}CD45RA^{-}$, T_{EM}) T-cells from healthy donors was analysed as
719 internal control (n=8).

720 Statistical significance was calculated using One way –ANOVA and reported as *p<0.05, **p<0.01,
721 ***p<0.001.

722

723 SUPPLEMENTARY FIGURE 2:

724 **A**: Frequencies of IFN-γ, TNF-α, GM-CSF (bar histograms) producing cells and co-expression of IL-
725 17A/IL-22 (right, stacked histogram) among *ex vivo* stimulated $CCR10^{+}CCR6^{+}TH22$- and $CCR10^{-}$
726 $CCR6^{SP}$ T-cell subsets of HDs (n=4). **B**: Representative images showing immunofluorescence of IL-
727 $10^{lo/-}$Th17-cells and IL-$10^{hi/+}$Tfh17-cells. **C**: Frequencies of $CCR10^{+}$ and $CCR10^{-}CCR6^{SP}$T-cell
728 subsets that expressed a functional IL-6R (centre) or IL-23R (right), as assessed by STAT3
729 phosphorylation in response to IL-6 and IL-23, respectively. Cells cultured without cytokines
730 ("UNSTIMULATED") are shown as control.

731

732 SUPPLEMENTARY FIGURE 3:

733 **A**: FACS-purified $CCR6^{SP}$-T-cells were stimulated with anti-CD3/CD28-coated beads in the absence
734 or presence of recombinant TGF-β, WNT10A, IL-4 or IL-12 as indicated. After 6 days cells were
735 restimulated with PMA and Ionomycin and production of IL-10 and IL-22 analysed. Statistical
736 significance was calculated by One-way ANOVA **B**: FACS dot plots of one representative experiment
737 showing IL-17 versus IFN-γ production by $CCR6^{SP}$-T-cells stimulated with anti-CD3/CD28-coated
738 beads in the absence or presence of IL-4 or IL-12. **C**: The day 6 culture supernatant of anti-
739 CD3/CD28-stimulated $CCR6^{+}$-T-cell subsets was analysed for IL-6 by ELISA (n=3). **D:** Dot plots of
740 one representative experiment showing $CCR6^{SP}$T-cells cultured with anti-CD3/28-coated beads in the
741 absence or presence of agents neutralizing IL-6, -10 and -21 and analyzed for IL-17 and IL-22
742 production.

743

744 SUPPLEMENTARY FIGURE 4:

745 **A**: Heatmap of median normalized expression of markers within each of the 16 clusters identified.
746 Dendrogram on the left side of the heatmap shows similarities among clusters. Red indicates high
747 and blue low expression. **B**: Histograms showing the expression levels of the 13 markers in the 16
748 $CD4^{+}$T-cell clusters. **C:** UMAPs showing the expression of the individual 13 markers. Red indicates
749 high, green intermediate and blue low expression levels. **D:** Frequencies of naïve
750 ($CD45RA^{+}CCR7^{+}CD95^{-}$) and memory T-cell subsets, i.e. Tscm ($CD45RA^{+}CCR7^{+}CD95^{+}$), Tcm
751 ($CCR7^{+}CD45RA^{-}$), Tem ($CCR7^{-}CD45RA^{-}$) and Temra ($CCR7^{-}CD45RA^{+}$) in HDs (blue bars) and

752 HIES patients (red bars). **E:** Frequencies of Th1- ($CD4^+CXCR3^+CCR4^-CCR6^-$) and Th2-cells
753 ($CD4^+CXCR3^-CCR4^+CCR6^+$), as well as Tregs ($CD4^+FOXP3^+IL\text{-}7R^{lo}$) and Tr1-cells
754 ($CD4^+GZMK^+IL\text{-}7R^{lo}$) in HD (blue bars, n=7) and AD-HIES patients (red bars, n=6).

755

756 SUPPLEMENTARY FIGURE 5:

757 **A:** Expression of CD27 and **B**: of CCR5 in $CCR6^+$ and $CCR6^-$T-cells of HIES patients (n=4) and
758 healthy donors (HD, n=4-8).

759

760 SUPPLEMENTARY FIGURE 6:

761 **A**: TNF-α and GM-CSF production by *ex vivo* stimulated $CCR6^+$ and $CCR6^-$ T-cell subsets of healthy
762 donors (HD, blue, n=7) and AD-HIES patients (red, n=4). **B**: IL-10 production by *ex vivo*–stimulated
763 T regulatory subsets from AD-HIES patients (red bars, n= 4-6) and healthy donors (blue bars, n=3-
764 4).

765

766 SUPPLEMENTARY FIGURE 7:

767 **A**: Expression of HLA-DR (left) and CD86 (right) by isolated $CD14^+$ monocytes from healthy donors
768 (n=3) incubated with the indicated heat killed pathogens. Statistical significance was calculated using
769 One way ANOVA and reported as *p<0.05, **p<0.01, ***p<0.001 vs unstimulated. **B**: Expression of
770 CD69 alone or together with IFN-γ, IL-2, IL-17A and IL-10 in $CCR6^+$ (upper panels) or $CCR6^-$
771 (lower panels) T-cells from HIES patients (red bars, n=5) and healthy donors (HD, blue bars, n=8) in
772 the absence (Unstim) or presence of SEB or LPS. Statistical significance was calculated using paired
773 t-test and reported as * $p < 0.05$. **C-E**: Co-expression of CD69 and the indicated cytokines in $CCR6^{+/-}$
774 T-cells from AD-HIES patients (red bars, n=4-5) and healthy donors (HD, blue bars, n=7-8) upon
775 stimulation with pathogen-derived antigens **C**: $CCR6^-$T-cells stimulated with the indicated heat-killed
776 pathogens **D**: $CCR6^+$(upper panels) or $CCR6^-$T-cells (lower panels) stimulated with overlapping
777 peptide pools derived from C. albicans (MP65) or Aspergillus (AMT). **E**: Co-expression of CD69
778 and IFN-γ in $CCR6^-CD4^+$T-cells from AD-HIES patients (red bars, n=4-5) and healthy donors (HD,
779 blue bars, n=8) stimulated with an EBV-derived peptide pool.

780

781 SUPPLEMENTARY TABLE 1: LIST OF ANTIBODIES

782

783 SUPPLEMENTARY TABLE 2: LIST OF ANTIGENS

784

785

786

787 **REFERENCES**

788

789 1. Geginat, J.*, et al.* The CD4-centered universe of human T cell subsets. *Semin Immunol* **25**, 252-262
790 (2013).
791 2. Crotty, S. Follicular helper CD4 T cells (TFH). *Annual review of immunology* **29**, 621-663 (2011).
792 3. Korn, T., Oukka, M., Kuchroo, V. & Bettelli, E. Th17 cells: effector T cells with inflammatory properties.
793 *Semin Immunol* **19**, 362-371 (2007).
794 4. Annunziato, F., Cosmi, L., Liotta, F., Maggi, E. & Romagnani, S. The phenotype of human Th17 cells
795 and their precursors, the cytokines that mediate their differentiation and the role of Th17 cells in
796 inflammation. *International immunology* **20**, 1361-1368 (2008).
797 5. Codarri, L.*, et al.* RORgammat drives production of the cytokine GM-CSF in helper T cells, which is
798 essential for the effector phase of autoimmune neuroinflammation. *Nature immunology* **12**, 560-567
799 (2011).
800 6. Singh, S.P.*, et al.* Human CCR6+ Th Cells Show Both an Extended Stable Gradient of Th17 Activity and
801 Imprinted Plasticity. *J Immunol* **210**, 1700-1716 (2023).
802 7. Zielinski, C.E.*, et al.* Pathogen-induced human TH17 cells produce IFN-gamma or IL-10 and are
803 regulated by IL-1beta. *Nature* **484**, 514-518 (2012).
804 8. Peters, A., Lee, Y. & Kuchroo, V.K. The many faces of Th17 cells. *Current opinion in immunology* **23**,
805 702-706 (2011).
806 9. Maggi, L.*, et al.* CD161 is a marker of all human IL-17-producing T-cell subsets and is induced by RORC.
807 *European journal of immunology* **40**, 2174-2181 (2010).
808 10. Paroni, M.*, et al.* An intestinal Th17 subset is associated with inflammation in Crohn's Disease and
809 activated by adherent-invasive Escherichia coli (AIEC). *J Crohns Colitis* (2023).
810 11. Acosta-Rodriguez, E.V.*, et al.* Surface phenotype and antigenic specificity of human interleukin 17-
811 producing T helper memory cells. *Nat Immunol* **8**, 639-646 (2007).
812 12. Paroni, M.*, et al.* Recognition of viral and self-antigens by TH1 and TH1/TH17 central memory cells in
813 patients with multiple sclerosis reveals distinct roles in immune surveillance and relapses. *J Allergy*
814 *Clin Immunol* (2017).
815 13. Duhen, T. & Campbell, D.J. IL-1beta promotes the differentiation of polyfunctional human
816 CCR6+CXCR3+ Th1/17 cells that are specific for pathogenic and commensal microbes. *Journal of*
817 *immunology* **193**, 120-129 (2014).
818 14. Duhen, T., Geiger, R., Jarrossay, D., Lanzavecchia, A. & Sallusto, F. Production of interleukin 22 but not
819 interleukin 17 by a subset of human skin-homing memory T cells. *Nat Immunol* **10**, 857-863 (2009).
820 15. Trifari, S., Kaplan, C.D., Tran, E.H., Crellin, N.K. & Spits, H. Identification of a human helper T cell
821 population that has abundant production of interleukin 22 and is distinct from T(H)-17, T(H)1 and
822 T(H)2 cells. *Nature immunology* **10**, 864-871 (2009).
823 16. Morita, R.*, et al.* Human blood CXCR5(+)CD4(+) T cells are counterparts of T follicular cells and contain
824 specific subsets that differentially support antibody secretion. *Immunity* **34**, 108-121 (2011).
825 17. Sallusto, F., Geginat, J. & Lanzavecchia, A. Central memory and effector memory T cell subsets:
826 function, generation, and maintenance. *Annu Rev Immunol* **22**, 745-763 (2004).
827 18. Rivino, L.*, et al.* Chemokine receptor expression identifies Pre-T helper (Th)1, Pre-Th2, and
828 nonpolarized cells among human CD4+ central memory T cells. *J Exp Med* **200**, 725-735 (2004).
829 19. Zhou, L.*, et al.* IL-6 programs T(H)-17 cell differentiation by promoting sequential engagement of the
830 IL-21 and IL-23 pathways. *Nature immunology* **8**, 967-974 (2007).
831 20. Kastirr, I.*, et al.* IL-21 Is a Central Memory T Cell-Associated Cytokine That Inhibits the Generation of
832 Pathogenic Th1/17 Effector Cells. *Journal of immunology* (2014).
833 21. Korn, T.*, et al.* IL-21 initiates an alternative pathway to induce proinflammatory T(H)17 cells. *Nature*
834 **448**, 484-487 (2007).
835 22. Asano, T.*, et al.* Human STAT3 variants underlie autosomal dominant hyper-IgE syndrome by negative
836 dominance. *J Exp Med* **218**(2021).

23. Tsilifis, C., Freeman, A.F. & Gennery, A.R. STAT3 Hyper-IgE Syndrome-an Update and Unanswered Questions. *J Clin Immunol* **41**, 864-880 (2021).
24. Milner, J.D.*, et al.* Impaired T(H)17 cell differentiation in subjects with autosomal dominant hyper-IgE syndrome. *Nature* **452**, 773-776 (2008).
25. Puel, A.*, et al.* Inborn errors of human IL-17 immunity underlie chronic mucocutaneous candidiasis. *Curr Opin Allergy Clin Immunol* **12**, 616-622 (2012).
26. Rivino, L.*, et al.* CCR6 is expressed on an IL-10-producing, autoreactive memory T cell population with context-dependent regulatory function. *J Exp Med* **207**, 565-577 (2010).
27. Facciotti, F.*, et al.* Evidence for a pathogenic role of extrafollicular, IL-10-producing CCR6(+)B helper T cells in systemic lupus erythematosus. *Proc Natl Acad Sci U S A* **117**, 7305-7316 (2020).
28. Cosmi, L.*, et al.* Human interleukin 17-producing cells originate from a CD161+CD4+ T cell precursor. *The Journal of experimental medicine* **205**, 1903-1916 (2008).
29. Carrabba, M.*, et al.* Long term longitudinal follow-up of an AD-HIES cohort: the impact of early diagnosis and enrollment to IPINet centers on the natural history of Job's syndrome. *Allergy Asthma Clin Immunol* **19**, 32 (2023).
30. Kastirr, I.*, et al.* Signal Strength and Metabolic Requirements Control Cytokine-Induced Th17 Differentiation of Uncommitted Human T Cells. *Journal of immunology* **195**, 3617-3627 (2015).
31. Moschetti, G.*, et al.* Deep Phenotyping of T-Cells Derived From the Aneurysm Wall in a Pediatric Case of Subarachnoid Hemorrhage. *Front Immunol* **13**, 866558 (2022).
32. Romagnani, S., Maggi, E., Liotta, F., Cosmi, L. & Annunziato, F. Properties and origin of human Th17 cells. *Molecular immunology* **47**, 3-7 (2009).
33. Rutitzky, L.I.*, et al.* IL-23 is required for the development of severe egg-induced immunopathology in schistosomiasis and for lesional expression of IL-17. *J Immunol* **180**, 2486-2495 (2008).
34. Gattinoni, L., Ji, Y. & Restifo, N.P. Wnt/beta-catenin signaling in T-cell immunity and cancer immunotherapy. *Clin Cancer Res* **16**, 4695-4701 (2010).
35. Lee, Y.S.*, et al.* The Wnt inhibitor secreted Frizzled-Related Protein 1 (sFRP1) promotes human Th17 differentiation. *Eur J Immunol* **42**, 2564-2573 (2012).
36. Majchrzak, K.*, et al.* beta-catenin and PI3Kdelta inhibition expands precursor Th17 cells with heightened stemness and antitumor activity. *JCI Insight* **2**(2017).
37. Annunziato, F.*, et al.* Phenotypic and functional features of human Th17 cells. *J Exp Med* **204**, 1849-1861 (2007).
38. Geginat, J.*, et al.* Plasticity of human CD4 T cell subsets. *Front Immunol* **5**, 630 (2014).
39. Ma, C.S.*, et al.* Deficiency of Th17 cells in hyper IgE syndrome due to mutations in STAT3. *J Exp Med* **205**, 1551-1557 (2008).
40. Geginat, J.*, et al.* Eomesodermin-expressing type 1 regulatory (EOMES(+) Tr1)-like T cells: Basic biology and role in immune-mediated diseases. *Eur J Immunol*, e2149775 (2023).
41. Geginat, J.*, et al.* IL-10 producing regulatory and helper T-cells in systemic lupus erythematosus. *Semin Immunol* **44**, 101330 (2019).
42. Gruarin, P.*, et al.* Eomesodermin controls a unique differentiation program in human IL-10 and IFN-gamma coproducing regulatory T cells. *Eur J Immunol* **49**, 96-111 (2019).
43. Pulvirenti, N.*, et al.* Characterization of human CD4(+) EOMES(+) GzmK(+) T-cell subsets unveils an uncoupling of suppressive functions from IL-10-producing capacities. *Eur J Immunol*, e2350675 (2024).
44. Facciotti, F.*, et al.* IL-10-producing forkhead box protein 3-negative regulatory T cells inhibit B-cell responses and are involved in systemic lupus erythematosus. *J Allergy Clin Immunol* **137**, 318-321 e315 (2016).
45. Haringer, B., Lozza, L., Steckel, B. & Geginat, J. Identification and characterization of IL-10/IFN-gamma-producing effector-like T cells with regulatory function in human blood. *J Exp Med* **206**, 1009-1017 (2009).
46. Minegishi, Y.*, et al.* Dominant-negative mutations in the DNA-binding domain of STAT3 cause hyper-IgE syndrome. *Nature* **448**, 1058-1062 (2007).
47. Steward-Tharp, S.M.*, et al.* A mouse model of HIES reveals pro- and anti-inflammatory functions of STAT3. *Blood* **123**, 2978-2987 (2014).

48. McGeachy, M.J., *et al.* TGF-beta and IL-6 drive the production of IL-17 and IL-10 by T cells and restrain T(H)-17 cell-mediated pathology. *Nat Immunol* **8**, 1390-1397 (2007).
49. Yang, L., *et al.* IL-21 and TGF-beta are required for differentiation of human T(H)17 cells. *Nature* **454**, 350-352 (2008).
50. Manel, N., Unutmaz, D. & Littman, D.R. The differentiation of human T(H)-17 cells requires transforming growth factor-beta and induction of the nuclear receptor RORgammat. *Nature immunology* **9**, 641-649 (2008).
51. Steinfelder, S., *et al.* Epigenetic modification of the human CCR6 gene is associated with stable CCR6 expression in T cells. *Blood* **117**, 2839-2846 (2011).
52. Canaria, D.A., *et al.* STAT5 Represses a STAT3-Independent Th17-like Program during Th9 Cell Differentiation. *J Immunol* **207**, 1265-1274 (2021).
53. Gagliani, N., *et al.* Th17 cells transdifferentiate into regulatory T cells during resolution of inflammation. *Nature* **523**, 221-225 (2015).
54. Xu, H., *et al.* The induction and function of the anti-inflammatory fate of TH17 cells. *Nat Commun* **11**, 3334 (2020).
55. Aschenbrenner, D., *et al.* An immunoregulatory and tissue-residency program modulated by c-MAF in human T(H)17 cells. *Nat Immunol* **19**, 1126-1136 (2018).
56. Freeman, A.F. & Holland, S.M. Clinical manifestations, etiology, and pathogenesis of the hyper-IgE syndromes. *Pediatr Res* **65**, 32R-37R (2009).
57. Wardlaw, A.J., Guillen, C. & Morgan, A. Mechanisms of T cell migration to the lung. *Clin Exp Allergy* **35**, 4-7 (2005).
58. Okada, S., *et al.* IMMUNODEFICIENCIES. Impairment of immunity to Candida and Mycobacterium in humans with bi-allelic RORC mutations. *Science* **349**, 606-613 (2015).
59. Giacomelli, M., *et al.* SH2-domain mutations in STAT3 in hyper-IgE syndrome patients result in impairment of IL-10 function. *Eur J Immunol* **41**, 3075-3084 (2011).
60. Geginat, J., *et al.* Reverse plasticity: TGF-beta and IL-6 induce Th1-to-Th17-cell transdifferentiation in the gut. *Eur J Immunol* **46**, 2306-2310 (2016).
61. Ma, C.S., *et al.* Unique and shared signaling pathways cooperate to regulate the differentiation of human CD4+ T cells into distinct effector subsets. *J Exp Med* **213**, 1589-1608 (2016).
62. Sabat, R., *et al.* Biology of interleukin-10. *Cytokine Growth Factor Rev* **21**, 331-344 (2010).
63. Paroni, M., *et al.* Uncontrolled IL-17 Production by Intraepithelial Lymphocytes in a Case of non-IPEX Autoimmune Enteropathy. *Clin Transl Gastroenterol* **7**, e182 (2016).

FIGURE 1

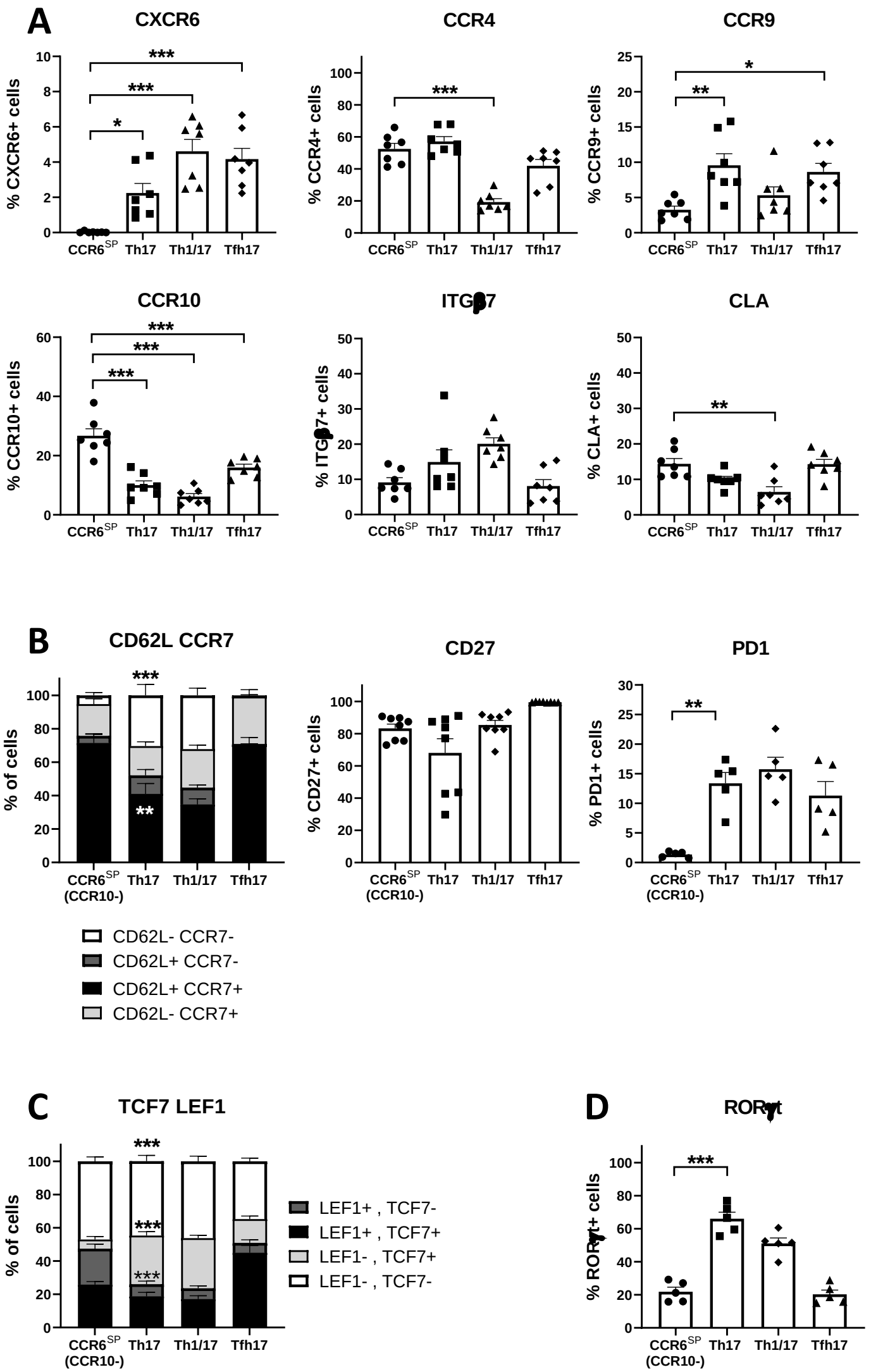
A
CXCR6
% CXCR6+ cells
CCR4
% CCR4+ cells
CCR9
% CCR9+ cells
CCR10
% CCR10+ cells
ITGβ7
% ITGβ7+ cells
CLA
% CLA+ cells
CCR6SP
Th17
Th1/17
Tfh17
B
CD62L CCR7
% of cells
CD27
% CD27+ cells
PD1
% PD1+ cells
CCR6SP (CCR10-)
CD62L- CCR7-
CD62L+ CCR7-
CD62L+ CCR7+
CD62L- CCR7+
C
TCF7 LEF1
% of cells
LEF1+ , TCF7-
LEF1+ , TCF7+
LEF1- , TCF7+
LEF1- , TCF7-
D
RORγt
% RORγt+ cells

FIGURE 2

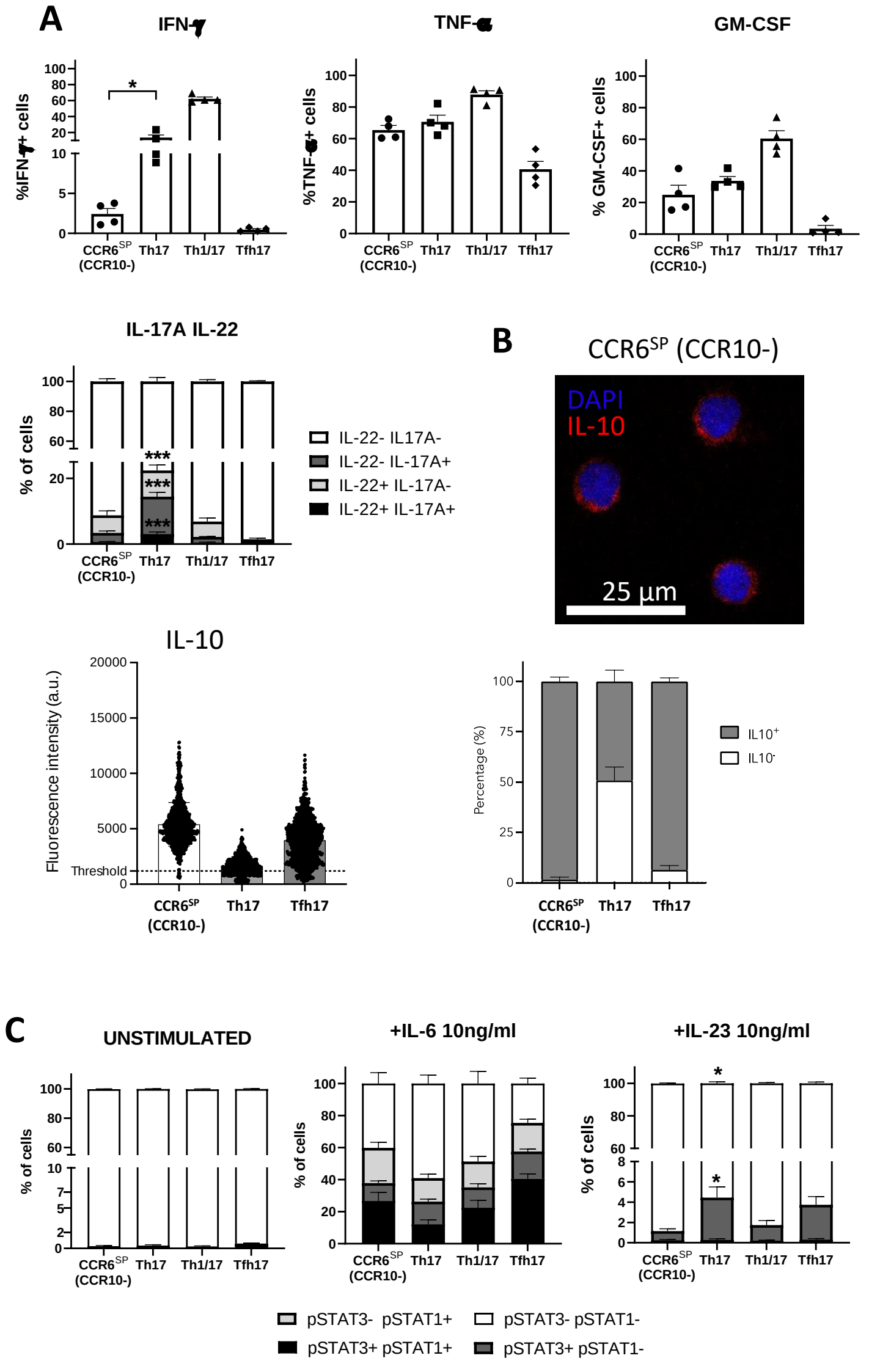
A
IFN-γ
TNF-α
GM-CSF
%IFN-γ+ cells
%TNF-α+ cells
% GM-CSF+ cells
CCR6SP (CCR10-)
Th17
Th1/17
Tfh17
IL-17A IL-22
% of cells
IL-22- IL17A-
IL-22- IL-17A+
IL-22+ IL-17A-
IL-22+ IL-17A+
B
CCR6SP (CCR10-)
DAPI
IL-10
25 µm
IL-10
Fluorescence intensity (a.u.)
Threshold
Percentage (%)
IL10+
IL10-
C
UNSTIMULATED
+IL-6 10ng/ml
+IL-23 10ng/ml
pSTAT3- pSTAT1+
pSTAT3- pSTAT1-
pSTAT3+ pSTAT1+
pSTAT3+ pSTAT1-

FIGURE 3

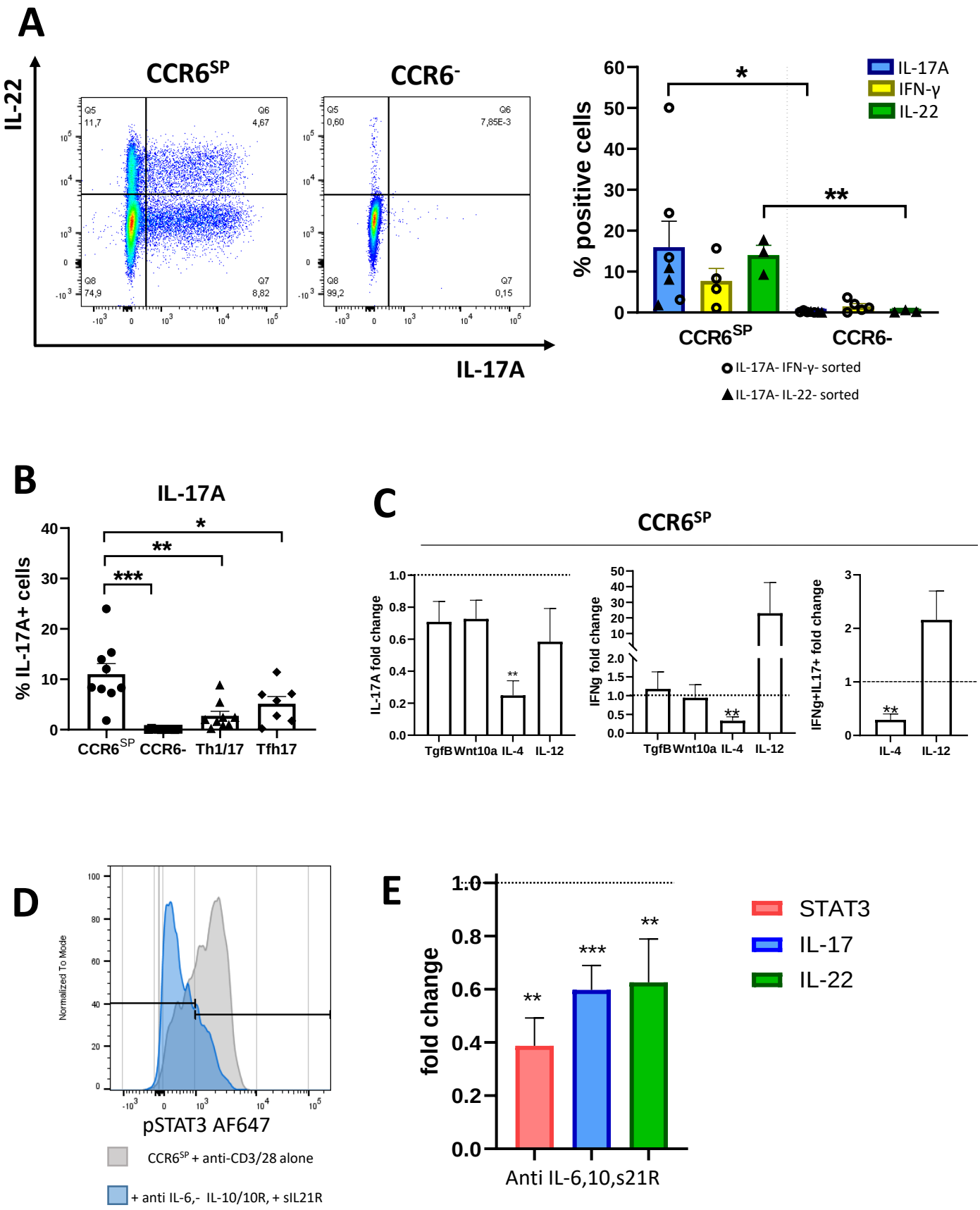
A
CCR6SP
CCR6-
IL-22
IL-17A
Q5 11,7
Q6 4,67
Q8 74,9
Q7 8,82
Q5 0,60
Q6 7,85E-3
Q8 99,2
Q7 0,15
% positive cells
IL-17A
IFN-γ
IL-22
CCR6SP
CCR6-
IL-17A- IFN-γ- sorted
IL-17A- IL-22- sorted
B
IL-17A
% IL-17A+ cells
CCR6SP
CCR6-
Th1/17
Tfh17
C
CCR6SP
IL-17A fold change
IFNg fold change
IFNg+IL17+ fold change
TgfB
Wnt10a
IL-4
IL-12
D
Normalized To Mode
pSTAT3 AF647
CCR6SP + anti-CD3/28 alone
+ anti IL-6,- IL-10/10R, + sIL21R
E
fold change
STAT3
IL-17
IL-22
Anti IL-6,10,s21R

FIGURE 4

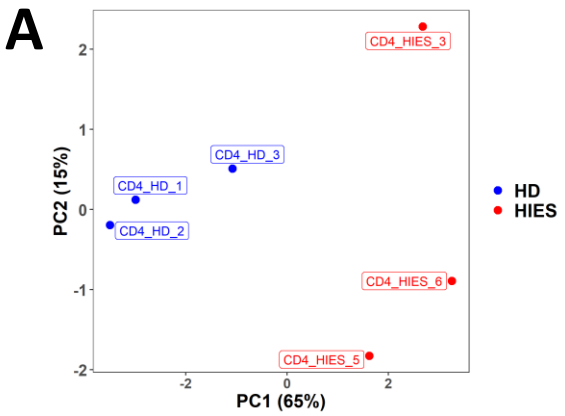
A
CD4_HIES_3
CD4_HD_3
CD4_HD_1
CD4_HD_2
CD4_HIES_6
CD4_HIES_5
PC2 (15%)
PC1 (65%)
HD
HIES

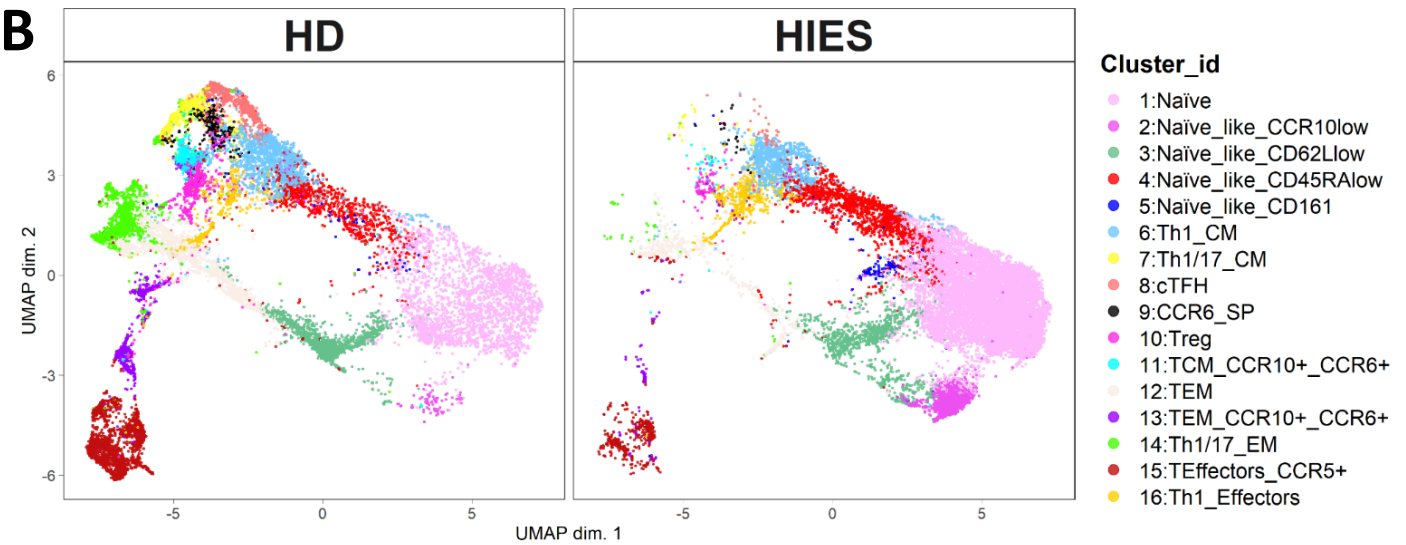
B
HD
HIES
UMAP dim. 2
UMAP dim. 1
Cluster_id
1:Naïve
2:Naïve_like_CCR10low
3:Naïve_like_CD62Llow
4:Naïve_like_CD45RAlow
5:Naïve_like_CD161
6:Th1_CM
7:Th1/17_CM
8:cTFH
9:CCR6_SP
10:Treg
11:TCM_CCR10+_CCR6+
12:TEM
13:TEM_CCR10+_CCR6+
14:Th1/17_EM
15:TEffectors_CCR5+
16:Th1_Effectors

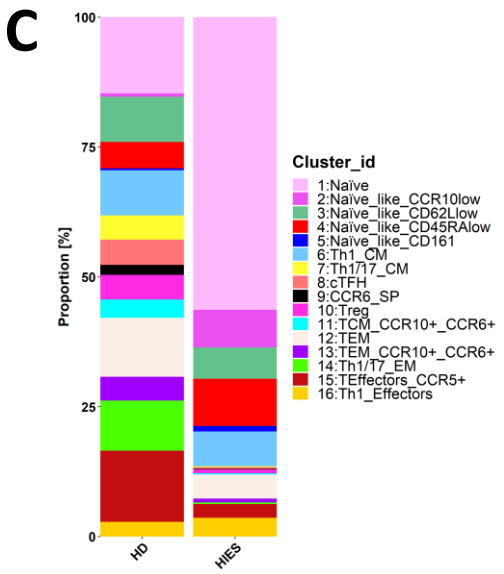
C
Proportion [%]
HD
HIES
Cluster_id
1:Naïve
2:Naïve_like_CCR10low
3:Naïve_like_CD62Llow
4:Naïve_like_CD45RAlow
5:Naïve_like_CD161
6:Th1_CM
7:Th1/17_CM
8:cTFH
9:CCR6_SP
10:Treg
11:TCM_CCR10+_CCR6+
12:TEM
13:TEM_CCR10+_CCR6+
14:Th1/17_EM
15:TEffectors_CCR5+
16:Th1_Effectors

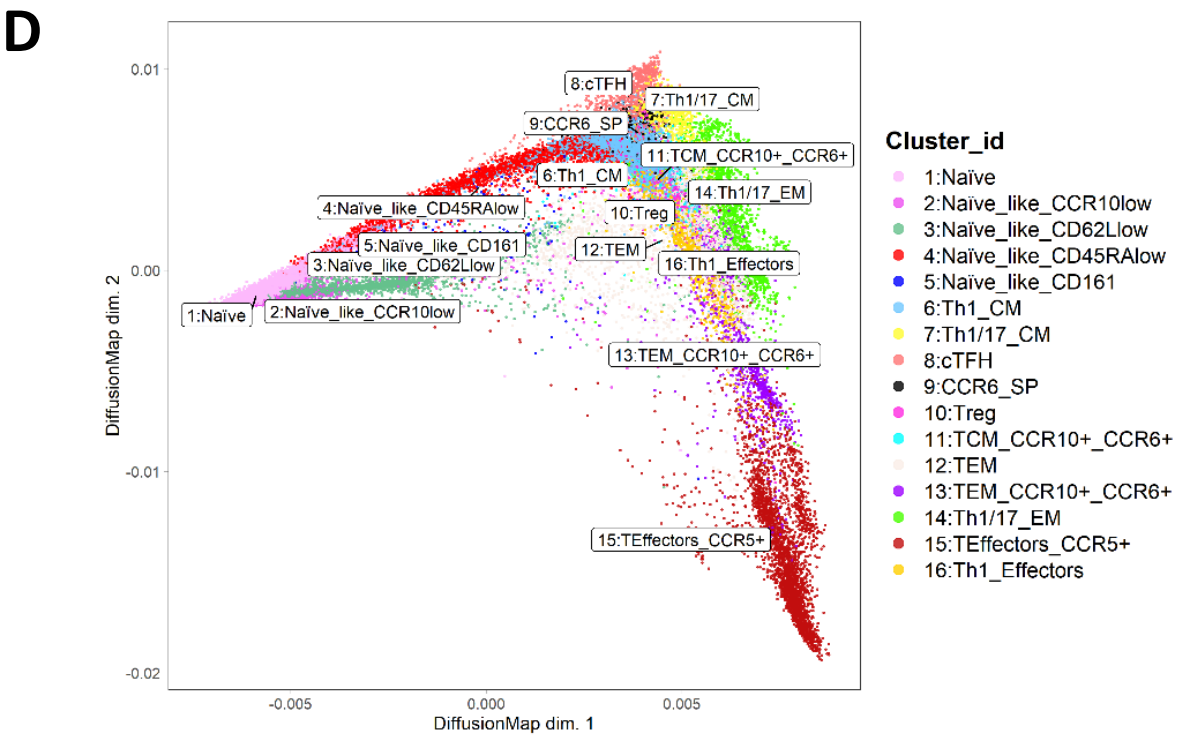
D
8:cTFH
7:Th1/17_CM
9:CCR6_SP
11:TCM_CCR10+_CCR6+
6:Th1_CM
14:Th1/17_EM
4:Naïve_like_CD45RAlow
10:Treg
5:Naïve_like_CD161
12:TEM
3:Naïve_like_CD62Llow
16:Th1_Effectors
1:Naïve
2:Naïve_like_CCR10low
13:TEM_CCR10+_CCR6+
15:TEffectors_CCR5+
DiffusionMap dim. 2
DiffusionMap dim. 1
Cluster_id
1:Naïve
2:Naïve_like_CCR10low
3:Naïve_like_CD62Llow
4:Naïve_like_CD45RAlow
5:Naïve_like_CD161
6:Th1_CM
7:Th1/17_CM
8:cTFH
9:CCR6_SP
10:Treg
11:TCM_CCR10+_CCR6+
12:TEM
13:TEM_CCR10+_CCR6+
14:Th1/17_EM
15:TEffectors_CCR5+
16:Th1_Effectors

FIGURE 5

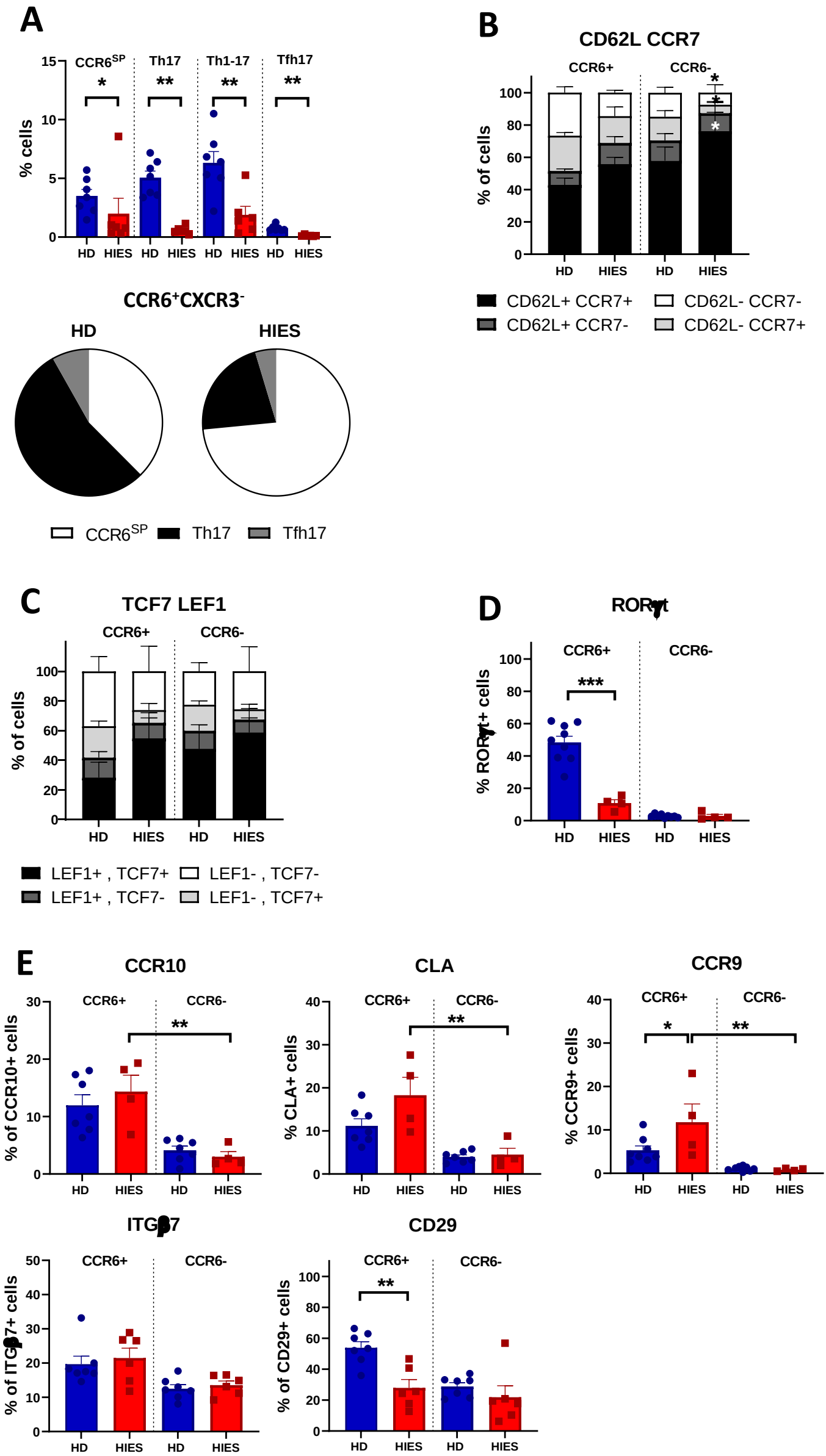
A
CCR6SP
Th17
Th1-17
Tfh17
% cells
HD HIES HD HIES HD HIES HD HIES
CCR6+CXCR3-
HD
HIES
CCR6SP Th17 Tfh17
B
CD62L CCR7
CCR6+
CCR6-
% of cells
HD HIES HD HIES
CD62L+ CCR7+
CD62L- CCR7-
CD62L+ CCR7-
CD62L- CCR7+
C
TCF7 LEF1
CCR6+
CCR6-
% of cells
HD HIES HD HIES
LEF1+ , TCF7+
LEF1- , TCF7-
LEF1+ , TCF7-
LEF1- , TCF7+
D
RORγt
CCR6+
CCR6-
% RORγt+ cells
HD HIES HD HIES
E
CCR10
CLA
CCR9
ITGβ7
CD29
% of CCR10+ cells
% CLA+ cells
% CCR9+ cells
% of ITGβ7+ cells
% of CD29+ cells
CCR6+
CCR6-
HD HIES HD HIES

FIGURE 6

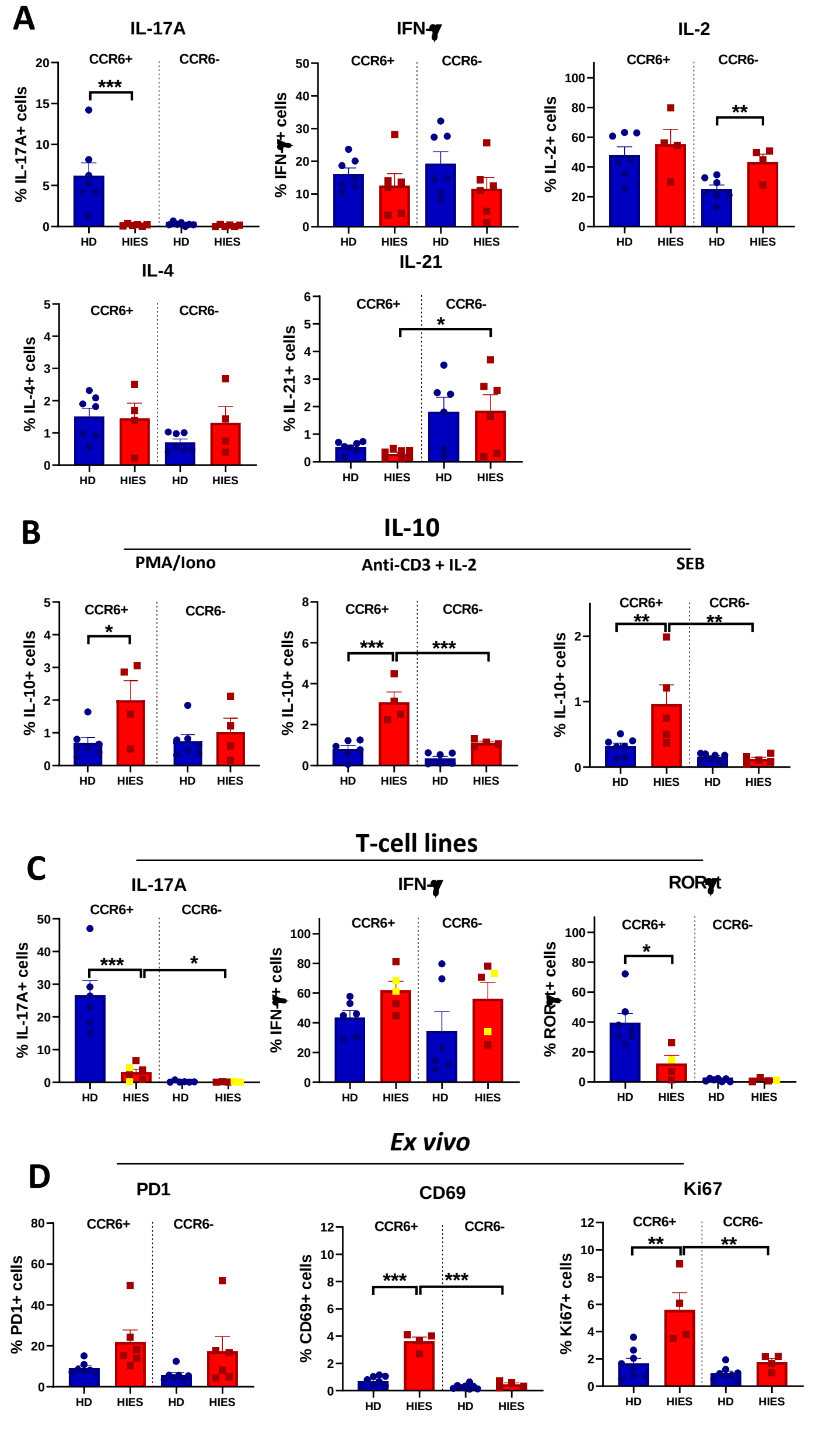
A
IL-17A
IFN-γ
IL-2
IL-4
IL-21
CCR6+
CCR6-
% IL-17A+ cells
% IFN-γ+ cells
% IL-2+ cells
% IL-4+ cells
% IL-21+ cells
HD
HIES
B
IL-10
PMA/Iono
Anti-CD3 + IL-2
SEB
% IL-10+ cells
C
T-cell lines
IL-17A
IFN-γ
RORγt
% IL-17A+ cells
% IFN-γ+ cells
% RORγt+ cells
D
Ex vivo
PD1
CD69
Ki67
% PD1+ cells
% CD69+ cells
% Ki67+ cells

FIGURE 7

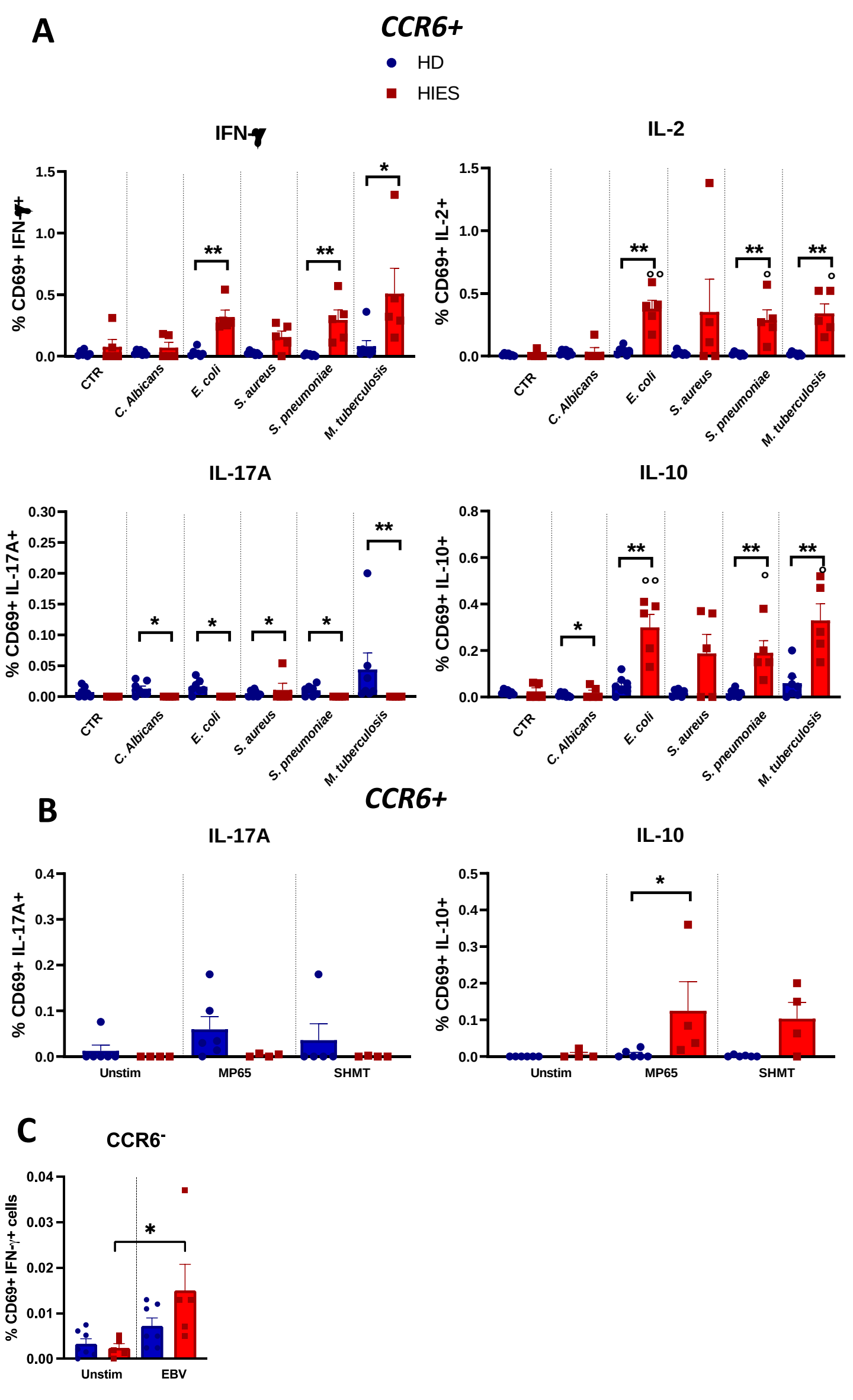
A
CCR6+
HD
HIES
IFN-γ
% CD69+ IFN-γ+
IL-2
% CD69+ IL-2+
IL-17A
% CD69+ IL-17A+
IL-10
% CD69+ IL-10+
CTR
C. Albicans
E. coli
S. aureus
S. pneumoniae
M. tuberculosis
B
CCR6+
IL-17A
% CD69+ IL-17A+
IL-10
% CD69+ IL-10+
Unstim
MP65
SHMT
C
CCR6-
% CD69+ IFN-γ+ cells
Unstim
EBV